Available online at www.sciencedirect.com
SCIENCE DIRECT®
Coordination Chemistry Reviews 248 (2004) 1565–1583
COORDINATION CHEMISTRY REVIEWS
www.elsevier.com/locate/ccr

Review

Allenylidene complexes of ruthenium: synthesis, spectroscopy and electron transfer properties☆

Rainer F. Winter[a,*], Stanislav Záliš[a,b]

[a] *Institut für Anorganische Chemie der Universität Stuttgart, Pfaffenwaldring 55, D-70569 Stuttgart, Germany*
[b] *J. Heyrovský Institute of Physical Chemistry, Academy of Sciences of the Czech Republic, Dolejškova 3, Prague, Czech Republic*

Received 6 January 2004
Available online 25 June 2004

Dedicated to William E. Geiger Jr. ("The Chief"), a great teacher and friend.

Contents

Abstract

This contribution deals with cationic ruthenium allenylidene complexes bearing a large variety of differently substituted allenylidene ligands attached to the metal. We discuss their synthesis and how the identity of the ER_n substituent influences their spectroscopic and electrochemical properties. It is shown, how data from different spectroscopies and electrochemical half-wave potentials relate to each others and provide a consistent picture of the bonding within these systems. Experimental results are compared to those from quantum mechanical studies.

Keywords: Allenylidene complexes of ruthenium; Spectroscopy; Electron transfer

1. Introduction

In 1970, E.O. Fischer published his seminal work on carbene complexes $[(CO)_5M{=}C(ER_n)(R')]$ of the chromium triad metals [1]. In systematically varying the substituents ER_n ($ER_n = NR_2$, OR, SR, SeR, aryl, alkyl) and R′ (R′ = aryl, alkyl) he and his co-workers were able to disclose, how substitution at the carbon end influences the physical and electronic properties of these systems [1–4]. Substituent ef-

☆ Supplementary data associated with this article can be found, in the online version, at doi:10.1016/j.ccr.2004.05.005.

* Corresponding author. Tel.: +49 711 685 4097; fax: +49 711 685 4165.
E-mail address: winter@iac.uni-stuttgart.de (R.F. Winter).

0010-8545/$ – see front matter © 2004 Elsevier B.V. All rights reserved.
doi:10.1016/j.ccr.2004.05.005

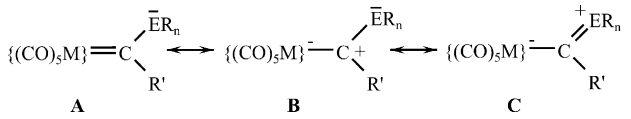

Plate 1.

fects were investigated by NMR and UV–vis spectroscopy, X-ray crystallography, dipole moment measurements and electrochemical techniques. During these studies the now well established dipolar character of these compounds as it is expressed in the zwitterionic resonance forms **B** and **C** (see Plate 1) and its variation with the nature of ER_n and R′ became evident.

We are summarizing here similar studies on allenylidene complexes of ruthenium(II). Allenylidene ligands are essentially cumulogous, more extended versions of carbenes and consist of three cumulated carbon atoms. Just like carbenes, they attach to the metal via a formal M=C double bond. The character of this bond, however, varies with the electronic properties of the substituents at the terminal carbon atom and those of the metal. The main focus of this account will be on the work done in our own laboratory on mostly the *trans*-$\{Cl(L_2)_2Ru\}^+$ entity where L_2 denotes a chelating diphosphine ligand [5], but results obtained by others and with related Ru(II) units will be discussed where appropriate. We wish to point out the intimate relationship between the Ru(II) units discussed here and the $(CO)_5M$ moieties utilized in the work of E.O. Fischer and the Constance group of H. Fischer. Both have a low-spin d^6 electronic configuration. The ruthenium entities may be considered as being more electron rich than the $M(CO)_5$ moieties but this is, at least in part, counterbalanced by the positive charge of the ruthenium complexes. Experimental and theoretical studies show indeed a strong parallelism between neutral $[(CO)_5M{=}C{=}C{=}CRR']$ and their cationic $[\{Ru\}{=}C{=}C{=}CRR']^+$ counterparts [5–11].

The subjects of this account are the following. (i) The synthesis of novel allenylidene complexes $[\{Ru\}{=}C{=}C{=}C(ER_n)(R')]^+$ with a broad range of heteroatom substituents ER_n (ii) Systematic studies on their spectroscopic, structural and electrochemical properties. Here it will be shown, how closely all the different properties relate to each others. Thus, individual parameters from different spectroscopies can be viewed as a manifestation of the subtle changes in the bonding within these complexes induced by the electronic properties of the allenylidene substituents and the other ligands at the metal atom. Some of the complexes have been constructed such that they bear electroactive substituents or ligands. These provide us with the opportunity to directly monitor the effects of changing the electron density on either the metal or the carbon end on the properties of these highly delocalized organometallic chromophores by simple redox chemistry. (iii) Results from quantum chemical studies that provide a sound basis for the interpretation of the experimental findings.

2. Synthesis of substituted allenylidene complexes from primary butatrienylidene intermediates

In studying longer chain pentatetraenylidene complexes *trans*-$[Cl(L_2)_2Ru{=}C{=}C{=}C{=}CAr_2]^+$, Touchard et al. [12,15] and Dixneuf and co-workers [12–15] observed the formation of stable, heteroatom substituted allenylidene complexes *trans*-$[Cl(L_2)_2Ru{=}C{=}C{=}C(ER_n)(CH{=}CAr_2)]^+$ from the regioselective addition of protic nucleophiles such as amines and alcohols to the internal $C_\gamma{=}C_\delta$ bond.[1] These reports were soon followed by similar observations of the Fischer group in Constance in their studies on bis(dimethylamino) substituted pentatetraenylidene or heptahexaenylidene complexes of chromium and tungsten [16–18]. Given the high aptitude of coordinatively unsaturated, electron-rich, cationic 16 valence electron complexes of ruthenium to isomerize terminal alkynes by formal 1,2-proton shift into vinylidene ligands [19–24], it was of interest to study their reactions with 1,3-diynes as a possible route to less well documented butatrienylidene complexes [25]. Most of this work was done with diacetylene (butadiyne) as the conceptually simplest and most reactive representative, first by the Adelaide group of Bruce [26–29] and then by us [5,11,30–36]. Despite considerable efforts there is still no direct proof for the existence of a primary butatrienylidene complex $[\{Ru\}{=}C{=}C{=}CH_2]^+$ ($\{Ru\} = Cp^RRu(PPh_3)_2$, *trans*-$Cl(L_2)_2Ru$). The outcome of all trapping reactions, however, support such a species as the reactive intermediate. The very recent isolation of thermally labile primary butatrienylidene complexes $[(\eta^5\text{-}C_5H_4R)(dmpe)Mn{=}C{=}C{=}CH_2]$ (R = Me, H; dmpe = $Me_2PC_2H_4PMe_2$) and their much more robust $SnPh_3$ substituted congeners by Berke and co-workers [37] lends further credibility to the existence of such species also in the ruthenium systems. The phenyl stabilized butatrienylidene complex *trans*-$[Cl(P^iPr_3)_2Ir{=}C{=}C{=}CPh_2]$ has been isolated and studied by Ilg and Werner [38]. We also note, that related butatrienylidene bridged diiron complexes $[Cp^*L_2Fe{=}C{=}C{=}C(E)\{Fe(CO)_2Cp^*\}]^+$ ($Cp^* = \eta^5\text{-}C_5Me_5$, E = H, Me, $L_2 = Ph_2PC_2H_4PPh_2$ (dppe) or $^iPr_2PC_2H_4P^iPr_2$ (dippe)) have been prepared by Lapinte et al. by treating the corresponding diynediyl complex with HBF_4 or MeOTf [39]. Cluster-stabilized primary butatrienylidene ligands are also known [40,41]. Our own observations led us to think that this species is just one component of a complex, equilibrating mixture of products arising from the interaction of the respective ruthenium species with butadiyne, but the most reactive one. In the presence of appropriate trapping agents it can be converted to a variety of products, often with good to excellent chemo- and regioselectivities.

[1] The carbon atoms along the cumulated ligands are counted such that the metal bonded carbon atom is denoted as C_α and subsequent atoms as C_β, C_γ and so on.

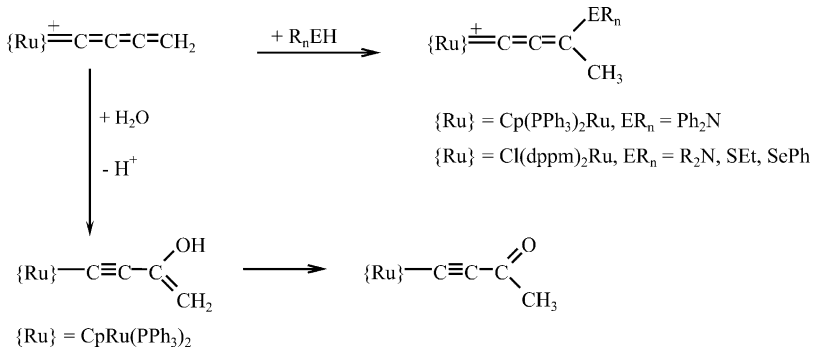

Scheme 1.

One principal reaction is their trapping with protic nucleophiles, which gives access to C-methylated, heteroatom substituted allenylidene complexes $[\{Ru\}{=}C{=}C{=}C(ER_n)(CH_3)]^+$. A broad variety of secondary amines [26,27,34], ethanethiol and phenyselenol [32] have been applied successfully (see Scheme 1). The latter reactions gave access to allenylidene complexes with previously unknown heteroatomic substitution. In contrast to similar pentatetraenylidene derivatives [12–15] and a related iron complex [42], alcohols proved to be unreactive toward the butatrienylidene species, possibly due to their lower nucleophilicity. With water, however, the keto substituted alkynyl complex $[Cp(PPh_3)_2Ru{-}C{\equiv}C{-}C(=O)(CH_3)]$ was obtained. Its formation was rationalized by a sequence involving regioselective water addition to carbon atom C_γ, deprotonation and tautomerization of the resulting enol [26,27]. In a like reaction, the acylvinylidene complex *trans*-$[Cl(dppe)Ru{=}C{=}C(H)\{C(=O)CH_2Ph\}]^+$ is formed by protonation of *trans*-$[Cl(dppe)_2Ru{-}C{\equiv}C{-}C{\equiv}CPh]$ with CF_3SO_3H, most likely via a secondary butatrienylidene species *trans*-$[Cl(dppe)_2Ru{=}C{=}C{=}C{=}CHPh]^+$ [43].

With pyrroles, formal CH-addition to the terminal $C_\gamma{=}C_\delta$ double bond is observed and results in pyrrolyl substituted allenylidene derivatives (Scheme 2) [26,27,44]. This reaction can also be viewed as an electrophilic attack on the electron-rich five-membered heterocycle by a $[\{Ru\}{=}C{=}C{=}C{=}CH_2]^+$ electrophile. The regioselectivity patterns consequently follow those observed for the electrophilic substitution of pyrroles known from organic chemistry. Thus, the positions neighbouring the pyrrole nitrogen atoms are generally more reactive than the remote 3 and 4 positions. The reaction of the putative *trans*-$[Cl(dppm)_2Ru{=}C{=}C{=}C{=}CH_2]^+$ with 2,5-dimethylpyrrole resulted in the 3-substituted pyrrolyl derivative rather than the NH-addition product [44]. A similar addition of pyrrol to the electron rich allenylidene complex $[Cp^*(dippe)Ru{=}C{=}C{=}C(Ph)(H)]^+$ afforded the functionalized chiral vinylidene complex $[Cp^*(dippe)Ru{=}C{=}CH{-}C(Ph)(H)(pyrrol\text{-}2\text{-}yl)]^+$ [45]. Pyrrolyl substituted allenylidene complexes display properties intermediate between those of amino and aryl substituted congeners and may thus be regarded as vinylogous aminoallenylidene complexes.

The addition of *N*,*N*-dimethylaminomethylferrocene follows a conceptually identical pathway. Primary addition of the amine to C_γ is followed by migration of the resonance stabilized ferrocenylmethyl carbenium ion to the neighbouring carbon atom C_δ. The $FcCH_2^+$ unit thus behaves as a proton equivalent (Scheme 3) [31].

Secondary amines were the most frequently used protic nucleophiles. As will be discussed later, the properties of the resulting aminoallenylidene complexes markedly depend on the electron richness (i.e. basicity) of the parent amine.

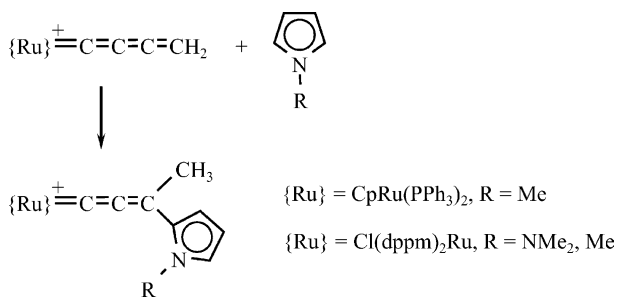

Scheme 2.

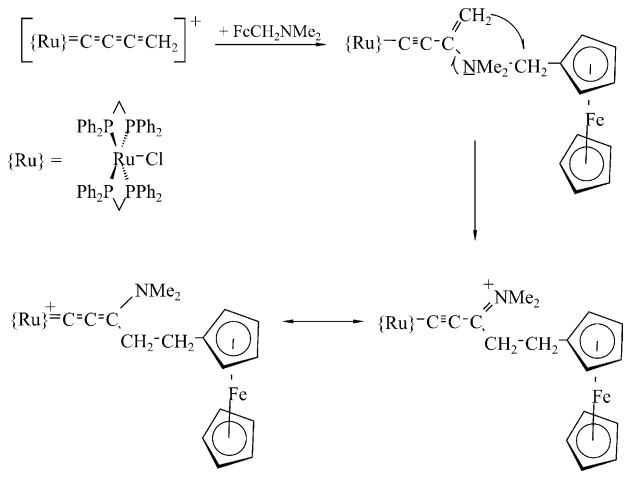

Scheme 3.

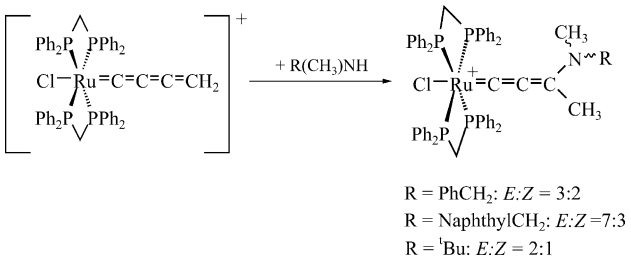

Scheme 4.

Unsymmetrically substituted secondary amines NRR′H give rise to *E*/Z isomeric mixtures (see Scheme 4). Individual isomers differ in which of the substituents points to the metal and which one away from it [34]. This requires a hindered rotation around the $C_\gamma N$ bond. The implications of this observation will be discussed in more detail in a later section.

A second general method for converting reactive butatrienylidene species into stable heteroatom substituted allenylidene complexes is their trapping by aprotic allyl substituted nucleophiles. The overall reaction involves nucleophilic attack, again on carbon atom C_γ, followed by Hetero-Cope (or -Claisen) rearrangement within the 3-hetero-1,5-diene subunit to give heteroatom substituted allenylidene complexes bearing a butenyl side chain (Scheme 5). These reactions were first observed for amines [11,30] and then for thio- and selenoethers [32,35] and provide rare examples of a sigmatropic rearrangement occurring within the coordination sphere of a transition metal complex [46]. In the case of allyl substituted amines, the simple adducts proposed as intermediates along the reaction paths were identified by virtue of a characteristic IR band near 2035 cm^{-1} ($\tilde{\nu}_{C\equiv C}$) and a ^{31}P NMR resonance close to −6 ppm. These values agree favourably with those for isolated ammoniobutenynyl complexes *trans*-$[Cl(dppm)_2Ru–C\equiv C–C(NR_2R')=CH_2]^+$, which were obtained from the reaction of the puatative *trans*-$[Cl(dppm)_2Ru=C=C=C=CH_2]^+$ with aliphatic or benzylic tertiary amines lacking an allyl functionality [30,33]. In the case of the propargylic amine $Me_2NCH_2C\equiv CH$, the simple adduct is thermally sufficiently stable to be isolated. This allowed its conversion to the rearranged aminoallenylidene isomer to be studied by ^{31}P NMR and UV–vis spectroscopy [33]. Following the reaction by ^{31}P NMR spectroscopy at elevated temperatures in different solvents showed little or no effect of the solvent polarity on the reaction rate.

We have recently shown, that electron rich aromatic five-membered heterocycles bearing a 2-dimethylaminomethyl substituent undergo essentially the same nucleophilic addition/rearrangement sequence as open chain aliphatic amines (Scheme 6). Thus, aminoallenylidene complexes with a 2-methylene-2,3-dihydrofuranyl, -thiophenyl or -selenophenyl substituent bonded to carbon atom C_γ were isolated [36]. A dimethylaminomethyl substituted thiazole and an isocyclic fulvalene react in the same manner (Scheme 6). These reactions differ from the more conventional Claisen-rearrangement of allyl substituted anilines or phenolethers in that the intracyclic double bond constitutes the allylic and not the vinylic component. Despite their comparative complexity and the concomitant loss of the aromaticity within the heterocyclic rings, all of these reactions require only simple starting materials and occur under surprisingly mild conditions, i.e. upon combining *cis*-$[RuCl_2(dppm)_2]$, $HC\equiv C–C\equiv CH$, $NaSbF_6$ as a mild halide abstracting agent and the respective amine in chlorobenzene or 1,2-dichlorobenzene and stirring for three to four days at ambient temperature. Warming or – even faster – proton catalysis effect tautomerization of the heterocyclic substituent to the 2-methyl substituted aromatic isomers as long as there is an additional proton attached to the carbon atom at the ring junction (Scheme 7). In the acid catalyzed case, we were able to characterize a protonated

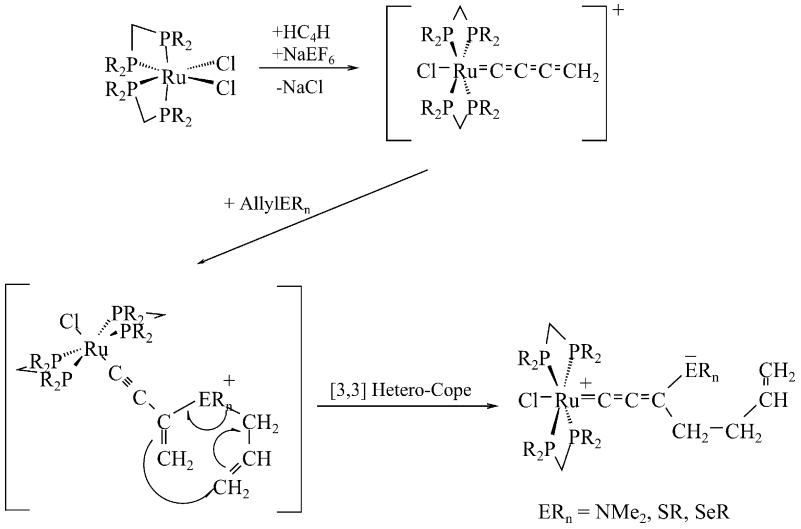

Scheme 5.

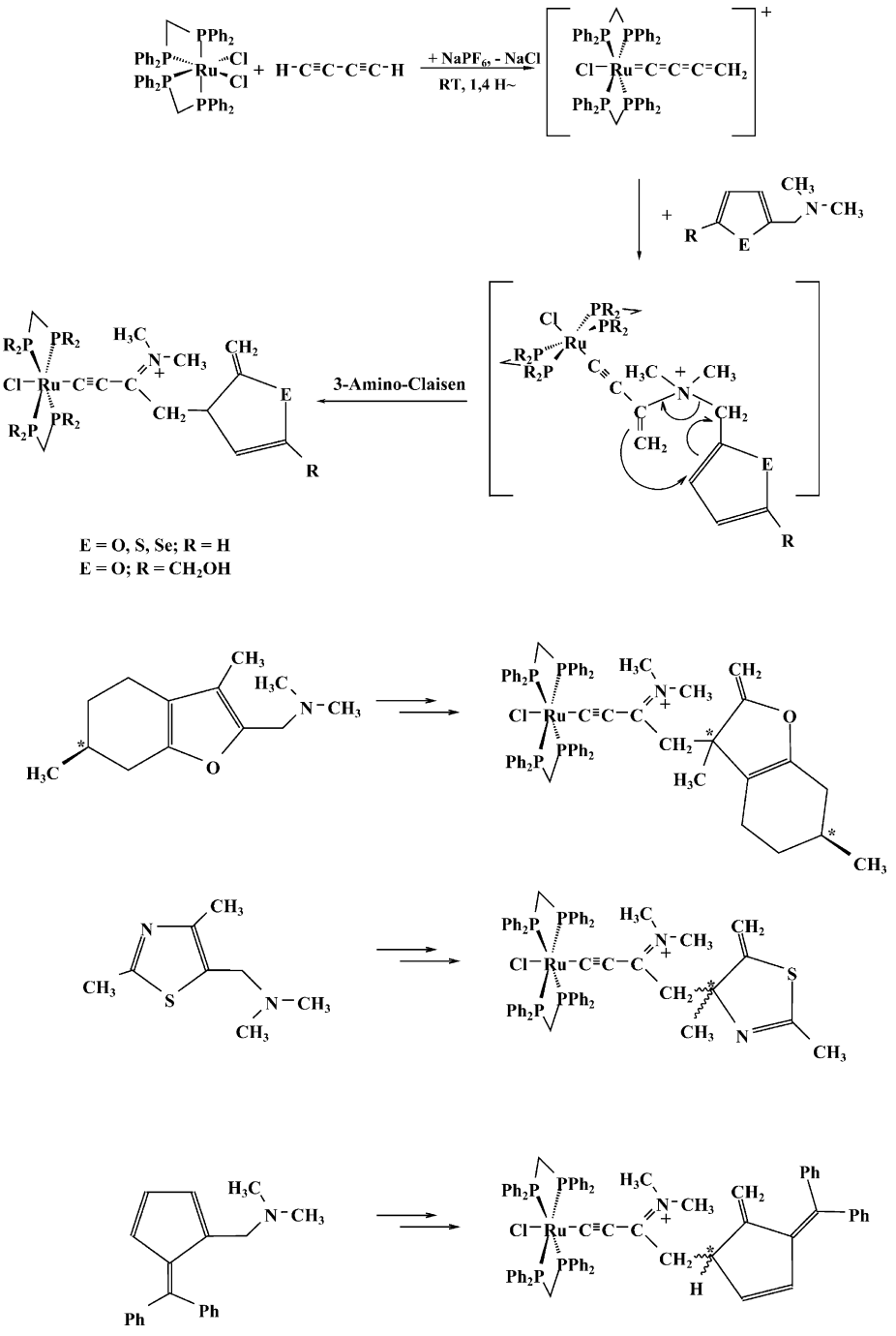

Scheme 6.

dicationic iminiumvinylidene (or aminocarbyne) species in the presence of stoichiometric amounts of a strong acid (Plate 2). Similar protonations have also been reported for aryl substituted allenylidene derivatives [10,45,47–49].

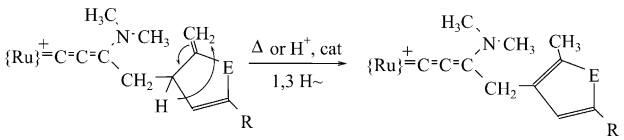

Scheme 7.

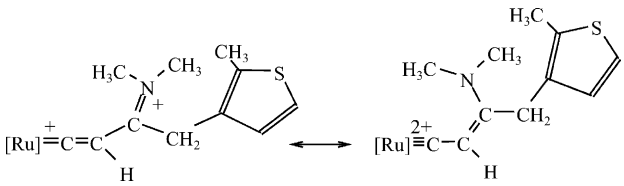

Plate 2.

Both principal methods of converting putative butatrienylidene species into heteroatom substituted allenylidene complexes allow for the introduction of just *one* heteroatomic substituent at the carbon terminus of the allenylidene ligand. Neutral allenylidene complexes of chromium and tungsten with two such substituents were recently obtained by Fischer and co-workers [16,50] and this elegant work will be detailed in another paper within this issue. To the best of our knowledge, no equivalent bis-donor substituted allenylidene complexes have been reported to date in ruthenium chemistry. Bis(alkyl), bis(aryl) or alkylaryl substituted congeners are, of course, easily available by treating the 16 valence electron precursors with the corresponding propargylic alcohol following Selegue's protocol [51].

According to calculations performed with the DFT approach [11], the high level of regioselectivity observed in all trapping reactions of the butatrienylidene species arises from a favourable combination of electronic and steric effects. Orbital coefficients at the LUMO, which is the orbital which controls the reactivity toward nucleophilic reagents, are equally high for all carbon atoms at odd positions along the cumulated chain. Carbon atoms at even positions of the C_4R_2-ligands contribute considerably less. Based on the orbital coefficients alone, rather unselective nucleophilic addition to either the carbon atoms C_α or C_γ would be expected. The metal bonded carbon atom C_α is, however, shielded by the bulky phosphine co-ligands at the metal which direct incoming nucleophiles to C_γ [10,11]. There are indeed cases for competing or even dominating addition to C_α in cationic allenylidene complexes containing sterically less demanding metal units [52–64]. A recent report by Rigaut et al. [65] on the unselective addition of hydride to both, the internal carbon atom C_γ and the terminal C_ε of a pentatetraenylidene complex emphasizes, that in longer chain cumulenylidene complexes the steric demand of the entering nucleophile may also play a role. We note again, that the calculational results for the *trans*-$\{Cl(PH_3)_4Ru\}^+$ and the $\{Cr(CO)_5\}$ derived model complexes are nearly identical [6,7,11]. This emphasizes the electronic equivalence of these two metal entities, even surpassing that expected from their isoelectronic relationship.

3. Properties of ruthenium allenylidene complexes

As one may expect of an extended delocalized chromophore, the properties of the allenylidene complexes critically depend on the substituents bonded to carbon atom C_γ and the other ligands at the metal. Here we will show, how close parameters from different spectroscopies relate to each others and how they combine to provide a consistent picture of the bonding within these systems.

Table 1
Comparison of the energies of the unsymmetrical CCC-stretch in complexes *trans*-$[Cl(dppm)_2Ru{=}C{=}C{=}C(ER_n)(R')]^+$ and the corresponding allenes $H_2C{=}C{=}C(ER_n)(R')$

ER_n	R′	$\tilde{\nu}_{as}$ $[\{Ru\}{=}C{=}C{=}C(ER_n)(R')]^+$ (cm^{-1})	$\tilde{\nu}_{as}$ $H_2C{=}C{=}C(ER_n)R'$ (cm^{-1})
Ph	Ph	1928	1938 [66]
Ph	Me	1938	1943 [67]
Me	Me	1964	1973 [66]
NR_2	Alkyl	1990–2000	1950 [68,69]
SR	Alkyl	1939–1943	1950 [70]
SeR	Alkyl	1930–1938	1950 [70]

3.1. IR spectroscopy

Cationic allenylidene complexes $[\{Ru\}{=}C{=}C{=}C(ER_n)(R')]^+$ can be described as a hybrid of four different resonance forms (**I–IV** in Plate 3): Two genuine cumulenic resonance forms with the positive charge on the metal (**I**) or C_α (**II**) and two alkynyl type resonance forms where the positive charge either resides at the terminal carbon atom (**III**) or at the ER_n moiety (**IV**). As the donor capacity of the ER_n group increases, resonance structures **III** and **IV** should be more favoured, especially so, when the E atom can donate a lone pair to the metallabutatriene π-system. The position of the asymmetric CCC stretch of the allenylidene ligand may thus serve as an at least qualitative measure for the contributions of the alkynyl versus the cumulenic resonance forms. This vibrational mode gives rise to a highly intense absorption for monocationic allenylidene complexes in the IR spectrum. In allenes, the corresponding band is also very intense and found in essentially the same spectral region. Table 1 compares the band energies of differently substituted allenylidene complexes *trans*-$[Cl(dppm)_2Ru{=}C{=}C{=}C(ER_n)(R')]^+$ and of the corresponding free allenes.

In heteroatom substituted allenes this band is invariably observed at 1950 cm^{-1}, independent of the exact nature of the heteroatom. In the corresponding allenylidene complexes, however, the position of this band varies between ca. 2000 cm^{-1} in amino substituted to about 1930 cm^{-1} in selenium substituted complexes with a clear trend toward lower energies for poorer donors. Within the series of amino substituted systems, for example, this band is found near 2000 cm^{-1} for derivatives of aliphatic amines but is shifted

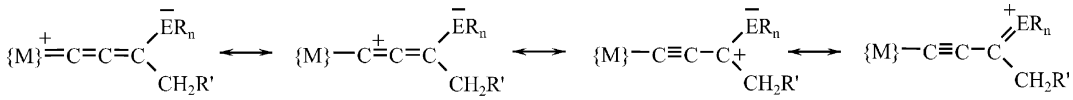

I II III IV

Plate 3.

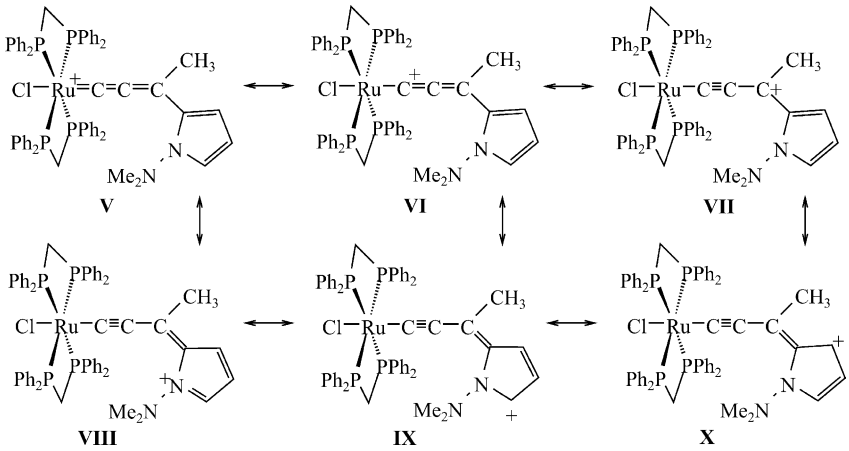

Plate 4.

to 1965 or 1941 wavenumbers for derivatives of the less basic iminostilbene or phenothiazine heterocycles [34]. In 2- or 3-substituted pyrrolyl derivatives, the electron rich heterocycle stabilizes the alkynyl type resonance forms **VII**–**X** (Plate 4). Here, the allenylidene band is found near 1955 cm^{-1} and thus at higher energies as is usually observed for aryl substituted systems (Table 1). Essentially the same trends were observed in the related half-sandwich allenylidene complexes $[(\eta^6\text{-}C_6Me_6)(L)ClRu{=}C{=}C{=}C(ER_n)(\text{–}CH{=}CPh_2)]^+$, where ER_n denotes NPh_2, OR (R = Et, ^{i}Pr) or phenyl and L is a phosphine ligand like PMe_3 or PMe_2Ph [12–14,53]. Similar observations were also reported by Tamm et al. for allenylidene complexes $[Cp(PPh_3)_2Ru{=}C{=}C{=}C(cht^R)]^+$ with a substituted cycloheptatrienylidene moiety (cht^R) bonded to the terminal carbon atom. In these latter complexes, the relative contributions of the alkynyl versus the cumulenic resonance forms were systematically altered via successive benzanelation or the introduction of peripheric phenyl groups [71]. Further examples can be found in the work of Touchard, who investigated aryl substituted allenylidene complexes $[Cl(dppm)_2Ru{=}C{=}C{=}C(Ph^R)_2]^+$ and $[Cl(dppm)_2Ru{=}C{=}C{=}C(Ph^R)(H)]^+$ with various *para* substituents attached to the phenyl rings. There is a notable decrease in the energy of the C=C=C stretch as the acceptor character of the aryl substituent increases [72]. Recently the group of H. Fischer has published several neutral allenylidene complexes of pentacarbonyl chromium and tungsten with a large variety of heteroatomic substituents bonded to C_γ [50]. As will be detailed in another paper within this issue, these complexes exhibit essentially the same behaviour as our cationic ruthenium based systems [73].

All experimental results point to a close relation between the position of this band and the order of the $C_\alpha C_\beta$ bond. Quantum chemical calculations on model complexes *trans*-$[Cl(PH_3)_4Ru{=}C{=}C{=}C\{(E(CH_3)_n\}(CH_3)]^+$ (E = N, *n* = 2, E = O, S, Se, *n* = 1) and *trans*-$[Cl(PH_3)_4Ru{=}C{=}C{=}C(R)(CH_3)]^+$ (R = Ph, Me) have indeed shown, that during this vibration carbon atoms C_α and C_β are strongly displaced from their equilibrium positions while the metal atom and C_γ exhibit only minor perturbations (Fig. 1). The asymmetric CCC mode therefore resembles a C≡C stretch of an alkyne (or, rather, an alkynyl complex) and its energy should thus reflect the order of the $C_\alpha C_\beta$ bond. A similar reasoning is applied for ketenes and diazo compounds, where a blue shift of the corresponding IR band is interpreted as indicating an increasing contribution of the zwitterionic resonance forms $RR'C^-\text{–}C{\equiv}O^+$ and $RR'C^-\text{–}N{\equiv}N^+$ [74]. Within a series of alkynyl complexes of the same metal entity, the energy of the C≡C stretch likewise decreases when the alkynyl ligand becomes a stronger acceptor. This is commonly viewed as arising from a higher contribution of the dipolar vinylidene resonance form $\{L_nM\}^+{=}C{=}CR^-$ [75–82].

A special position of aminoallenylidene complexes within this series is already evident from IR spectroscopy. According to the comparatively high energy of the allenylidene band, they are intermediate between acceptor substituted alkynyl complexes on one hand ($\tilde{\nu}_{CCC}$ = 2045 cm^{-1} for

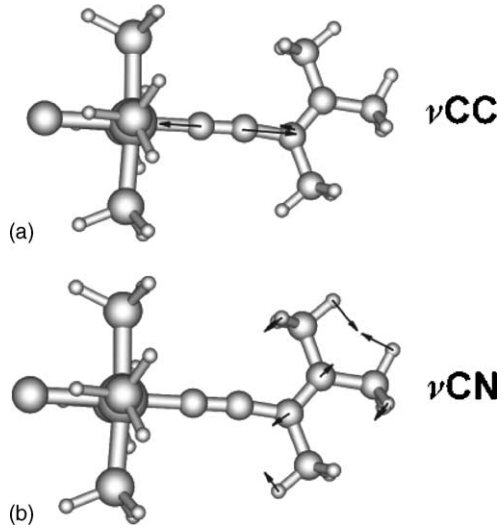

Fig. 1. Calculated atomic displacements for *trans*-$[Cl(PH_3)_4Ru{=}C{=}C{=}C(CH_3)(NMe_2)]^+$ for the vibrations at (a) 1995 cm^{-1} and (b) 1524 cm^{-1} (energies calculated after scaling).

trans-[Cl(dppm)$_2$Ru–C≡C–C$_6$H$_4$–NO$_2$-4] [82] and aryl substituted allenylidene complexes on the other, which generally have the highest cumulenic character ($\tilde{\nu}_{CCC}$ = 1921 cm^{-1} for *trans*-[Cl(dppm)$_2$Ru=C=C=C(C$_6$H$_4$Cl-4]$^+$) [72]. IR-spectroscopy provides further evidence for a significant contribution of the iminium alkynyl type resonance form **IV** in Plate 3. All aminoallenylidene complexes display an additional band of medium intensity at about 1550–1580 cm^{-1} which is absent in similar complexes having other ER$_n$ substituents. The position of this band correlates with the basicity of the parent amine and, like the allenylidene band itself, shifts to lower energy as the donor capacity of the NR$_2$ unit decreases. It is thus found at ca. 1490 cm^{-1} for the phenothiazine and iminostilbene derivatives [34]. This is highly reminiscent of the related aminocarbene complex [Cp(CO)(P^{i}Pr$_3$)Ru=C(NRR′)–CH=CPh$_2$]$^+$, which according to experimental and theoretical work is more adequately described in the azoniabutadienyl resonance form [Cp(CO)(P^{i}Pr$_3$)RuC(=NRR′)$^+$–CH=CPh$_2$] [56]. This complex also has an IR absorption at 1550 cm^{-1} which is ascribed to the C=N double bond vibration. Similar observations have been reported for neutral aminocarbene complexes of chromium and tungsten [83–85]. DFT-calculations on the simplified PH$_3$ model of our real complexes fully agree with this view [11]. As is depicted in Fig. 1, the underlying vibration is not a simple C=N stretch, but also involves a fair amount of angular distortions. The calculated energy of 1524 cm^{-1} matches the experimental values well.

The presence of a partial C=N multiple bond also gives rise to a sizable energy barrier for CN rotation. Thus, *E*/*Z* isomeric mixtures of *trans*-[Cl(dppm)$_2$Ru=C=C=C(NRR′)(CH$_3$)]$^+$ are formed when secondary amines with two different substituents are employed in the trapping of butatrienylidene intermediates (Scheme 4). In the case of *trans*-*E*/*Z*-[Cl(dppm)$_2$Ru=C=C=C(N^{t}BuMe)(CH$_3$)]$^+$, the separate singlets for the *E* and the *Z* isomer in the ^{31}P NMR spectrum were seen to coalesce at T = 398 K. This allowed us to derive energy barriers of 86.4 for the $E \rightarrow Z$ and of 84.1 kJ/mol for the $Z \rightarrow E$ isomerizations [34]. These energy barriers compare well to those observed for donor substituted iminium salts like Me$_2$N(EMe)C=NMe$_2^+$ (E = O, S) [86]. Quantum chemical calculations on the issue of the C=NRR′ rotation were performed on the modified model complex *trans*-[Cl(dhpm)$_2$Ru=C=C=C(NMe$_2$)(CH$_3$)]$^+$ (dhpm = H$_2$PCH$_2$PH$_2$). This model retains the angular distortions of the coordination environment of the metal imposed by the four membered diphosphine chelate while lacking the steric repulsion due to the phenyl substituents. They revealed that the observed barrier is electronic rather than steric in origin. The energy difference between the optimized structures for a parallel and an orthogonal orientation of the NR$_2$ entity with respect to the allenylidene π-system amounts to 109 kJ/mol. This is in good qualitative agreement with the experimental value for the HN^{t}BuMe derivative, especially when considering that in the dppm substituted real complexes steric hindrance between the bulky phosphine co-ligands and the NMe-group pointing toward the metal centre induce some torsion of the NMe$_2$ substituent out of the ClRuC$_3$N plane. Moreover, rotation induces a pyramidalization of the nitrogen atom and a lengthening of the C–N bond by about 9 pm as the organometallic π-system and the nitrogen lone pair are electronically decoupled [34].

3.2. X-ray crystallography

From a structural viewpoint, a higher contribution of alkynyl type resonance forms **III** and **IV** implies longer Ru–C$_\alpha$ and C$_\beta$–C$_\gamma$ as well as shorter C$_\alpha$–C$_\beta$ and C$_\gamma$–heteroatom bonds. Unfortunately, knowledge of the structures of ruthenium allenylidene complexes is largely restricted to amino and aryl substituted derivatives. Only one example of an alkoxy vinyl substituted congener has been crystallized to date, while no experimental studies of SR or SeR substituted complexes are known. Table 2 provides an overview of those ruthenium allenylidene complexes that have been studied by X-ray crystallography to date. Only complexes with coordinatively saturated ruthenium centers are considered.

A closer inspection of the data in Table 2 reveals, that the Ru–C bond of aminoallenylidene complexes (1.93–1.97 Å) is consistently longer than that in aryl substituted derivatives (1.83–1.92 Å). There is also a tendency toward shorter C$_\alpha$–C$_\beta$ and longer C$_\beta$–C$_\gamma$ bonds with average values of 1.225(5) and 1.403(9) Å for the amino substituted systems as compared to 1.254(8) and 1.349(13) Å in the aryl substituted ones (only those data, where the standard deviations are equal or less to 1% of the bond lengths were considered, values in brackets represent the variance of the average value). Partial or total substitution of aryl versus alkyl substituents seems to have only a small effect, although there are only relatively few data available for alkyl substituted congeners. The X-ray structures of amino substituted allenylidene complexes provide further evidence for a significant, or even dominating, contribution of the iminium alkynyl type resonance form, as has already been discussed in previous sections. Most notable are the invariably planar coordination of the nitrogen atom in all of the structures and a significant shortening of the C$_\gamma$–N bond by some 14–16 pm when compared to the NR and the NR′ bonds.

Amino substituted derivatives on one hand and aryl or alkyl substituted ones on the other represent the extremes within the series of allenylidene complexes, while derivatives with different heteroatomic substituents like OR, SR or SeR are at an intermediate position along a continuum between the more alkynyl and the more cumulenic C$_3$R(ER$_n$) ligands. One should, however, bear in mind that significant contributions of the alkynyl type resonance forms are to be discussed even for all carbon substituted derivatives [101]. In lieu of structural data for allenylidene complexes *trans*-[Cl(L$_2$)$_2$Ru=C=C=C(ER$_n$)(R′)]$^+$ with

Table 2
X-ray structure data for ruthenium allenylidene complexes: bond lengths

{Ru}	R	ER′R″	RuCα	CαCβ	CβCγ	CγE	CγR	ER′	ER″	Ref.
$\{ClRu(dppm)_2\}^+$	1-Butenyl	NMe_2	1.950(4)	1.218(6)	1.418(8)	1.244(8)	1.499(7)	1.505(7)	1.495(6)	[30]
$\{ClRu(dppe)_2\}^+$	1-Butenyl	NMe_2	1.934(8)	1.232(13)	1.393(13)	1.320(12)	1.544(18)	1.460(11)	1.466(13)	[10]
$\{ClRu(dppm)_2\}^+$	Me	NBzMe[l]	1.944(6)	1.223(9)	1.397(9)	1.290(10)	1.524(12)	1.430(12)	1.510(9)	[34]
$\{ClRu(dppm)_2\}^+$	CH_2-2-Me-thienyl	NMe_2	1.942(9)	1.228(11)	1.405(12)	1.309(12)	1.508(14)	1.456(13)	1.477(11)	[36]
$\{CpRu(PPh_3)_2\}^+$[a]	Me	NPh_2	1.94(1)	1.22(2)	1.36(2)	1.33(2)	1.50(2)	–	–	[27]
			1.97(1)	1.18(2)	1.41(2)	1.34(2)	1.50(2)	–	–	
$\{IndRu(PPh_3)_2\}^+$[b]	CH=CMe–CMe=CPh_2	NEt_2	1.946(4)	1.229(5)	1.390(5)	1.319(5)	1.500(5)	–	–	[87]
cis-$RuCl_2np_3$[c]	CH=CPh_2	OMe	1.921(5)	1.257(4)	1.369(7)	1.332(8)	1.443(8)	1.435(11)	–	[88]
$\{CpRu(PPh_3)_2\}^+$	Me	1-Methyl-pyrrol-2-yl	1.92(1)	1.24(2)	1.37(2)	1.40(2)	1.49(1)	–	–	[27]
$\{CpRu(PMe_3)_2\}^+$	Ph	Ph	1.884(5)	1.255(8)	1.329(9)	1.462(9)	1.511(8)	–	–	[51]
$\{Cp^*Ru(PEt_3)_2\}^+$	Ph	Ph	1.876(5)	1.245(7)	1.352(8)	1.463(7)	1.493(8)	–	–	[89]
$\{Me_3IndRu(CO)\text{-}(PPh_3)\}^+$[d]	Ph	Ph	1.92(1)	1.26(1)	1.35(2)	1.47(2)	1.48(2)	–	–	[90]
$\{IndRu(PPh_3)_2\}^+$[b]	Ph	Ph	1.878(5)	1.260(7)	1.353(7)	1.469(9)	1.475(8)	–	–	[8]
$\{tripodP_2Ru\}^+$[e]	Ph	Ph	1.892	1.270(8)	1.358(8)	–	–	–	–	[91]
$\{(p\text{-Cymen})Ru\text{-}(PPh_3)Cl\}^+$	Ph	Ph	1.894(3)	1.253(5)	1.361(5)	–	–	–	–	[92]
$\{(C_6H_5C_2H_4\text{-}PPh_2)RuCl\}^+$	Ph	Ph	1.903(4)	1.244(5)	1.364(5)	–	–	–	–	[92]
$\{TpRu(PPh_3)_2\}^+$[f]	Ph	Ph	1.889(3)	1.248(4)	1.357(4)	1.477(3)	1.481(3)	–	–	[93]
{TpRu(dppf)}[f,g]	Ph	Ph	1.88(4)	1.26(5)	1.32(5)	1.46(5)	1.52(5)	–	–	[34]
$\{cis\text{-}RuCl\text{-}(P^iPrOMe)_2\}^+$[h]	Ph	Ph	1.829(6)	1.259(9)	1.352(9)	1.484(8)	1.466(8)	–	–	[94]
$RuCl_2(\kappa^1\text{-}P{\sim}O)\text{-}(\kappa^2\text{-}P{\sim}O)$[i]	Ph	Ph	1.84(1)	1.27(2)	1.34(2)	1.45(2)	1.47(2)	–	–	[58]
$\{RuCl_2(\kappa^2\text{-}P'{\sim}O)\text{-}(\kappa^2\text{-}P'{\sim}O)]\}^+$[j]	Ph	Ph	1.840(3)	1.273(4)	1.357(4)	–	–			[95]
$Cl_2Ru(CO)(Sb^iPr_3)_2$	Ph	Ph	1.88(2)	1.24(2)	1.34(2)	–	–	–	–	[96]
$\{ClRu(dppm)_2\}^+$	3-Phenylinden-1-yliden		1.85(2)	1.29(3)	1.39(3)	1.43(4)	1.41(3)	–	–	[15]
$\{ClRu(dppm)_2\}^+$	Me	Ph	1.894(4)[m]	1.257(6)	1.346(6)	1.469(6)	1.508(6)			[5]
			1.886(6)[n]	1.267(8)	1.364(8)	1.470(8)	1.515(8)			
$\{Cp^*Ru(dippe)\}^+$[j]	Me	Ph	1.884(5)	1.257(6)	1.338(7)	1.460(6)	1.510(7)	–	–	[97]
$\{ClRu(dppm)_2\}^+$[a]	H	Ph	1.886(10)	1.254(14)	1.34(2)	1.42(2)	–	–	–	[98]
			1.874(11)	1.239(14)	1.36(2)	1.46(2)	–	–	–	
$\{Cp^*Ru(dippe)\}^+$[k]	H	Ph	1.865(8)	1.249(10)	1.320(12)	1.452(14)	–	–	–	[99]
$\{IndRu(PPh_3)_2\}^+$	4-Spirocyclohexan-bicyclo-[3.3.1]-non-2-en-9-yliden		1.889(5)	1.256(7)	1.339(7)	–	–	–	–	[100]

[a] Two independent molecules in the unit cell.
[b] Ind = η^5-Indenyl, η^5-C_9H_7.
[c] np_3 = $N(CH_2CH_2PPh_2)_3$.
[d] Me_3Ind = η^5-1,2,3-Trimethylindenyl, η^5-$C_9H_4Me_3$.
[e] $tripodP_2$ = $H_3CC(\eta^5\text{-}C_5H_4)(CH_2\text{-}\eta^1\text{-}PPh_2)_2$.
[f] Tp = Hydridotris(pyrazolyl)borate.
[g] dppf = 1,1′-bis(diphenylphosphino)ferrocene.
[h] P^iPrOMe = $^iPr_2PC_2H_4OMe$.
[i] P∼O = $^iPr_2PC_2H_4C(O)OMe$.
[j] P′∼O = $Cy_2PC_2H_4OMe$.
[k] dippe = $^iPr_2PC_2H_4P^iPr_2$.
[l] Bz = Benzyl.
[m] SbF_6^- salt measured at 298 K.
[n] PF_6^- salt measured at 173 K.

Table 3
Structural parameters of allenylidene complexes *trans*-$[Cl(PH_3)_4RuC_3\{E(CH_3)_n\}(CH_3)]^+$ as calculated by DFT methods

$E(CH_3)_n$/bond	$N(CH_3)_2$	OCH_3	SCH_3	$SeCH_3$	CH_3
Ru–Cl	2.470	2.460	2.512	2.513	2.461
Ru–P	2.349	2.357	2.422	2.425	2.370
Ru–C_α	1.957	1.936	1.937	1.929	1.921
C_α–C_β	1.256	1.261	1.263	1.269	1.268
C_β–C_γ	1.379	1.360	1.359	1.356	1.348
C_γ–$C(CH_3)$	1.504	1.499	1.503	1.507	1.498
C_γ–E	1.347 (N)	1.338 (O)	1.738 (S)	1.904 (Se)	1.498 (C)
E–C	1.468	1.450	1.887	1.996	–

other heteroatom substituents, we have undertaken quantum mechanical studies on permethylated model complexes ($R = R' = Me$) with four PH_3 instead of two diphosphine ligands. Relevant bond lengths for the optimized structures are provided in Table 3. Calculated parameters for the amino and methyl substituted congeners agree favourably to the experimental ones with a slightly long C_α–C_β and short C_β–C_γ bond. Substitution of the NR_2 by the OR, SR or SeR moiety leads to a successive lengthening of the C_α–C_β and shortening of the Ru–C_α and the C_β–C_γ bond, which indicates an increasing cumulenic character of the allenylidene ligand. This systematic trend retraces the shift of the allenylidene band observed in IR spectroscopy. One notes, however, that the changes in C–C bond lengths upon substitution are quite small. They may well be outside the accuracy that can be achieved with X-ray crystallography, especially when considering, that the bond lengths within the unsaturated carbon chain usually suffer from rather large standard deviations. Experimentally determined structural parameters, albeit highly desirable, may thus be less useful than the spectroscopic fingerprints for a meaningful discussion of the bonding in these allenylidene complexes.

3.3. Optical spectroscopy

An immediately apparent property of the allenylidene complexes is their highly intense coloration ranging from yellow green for amino and alkyl to intense green for thio, orange brown for seleno and violet to purple for aryl substituted derivatives. Fig. 2 displays the typical absorption spectra for a prototypical amino and a seleno substituted derivative. Nonwithstanding the shift of the respective absorption bands, all spectra exhibit an identical pattern of a highly intense absorption band near 400–480 nm and a much weaker, lower energy band near 600–700 nm. These bands have been assigned as arising from the HOMO-1 → LUMO and the HOMO → LUMO transitions. The HOMO → LUMO transition is symmetry forbidden, which explains the low intensity of the corresponding absorption band, while the excitation from the lower lying HOMO-1 level is symmetry allowed [11]. Independent of the respective ER_n substituent ($ER_n = CH_3$, NMe_2, OMe, SMe, SeMe) [5], both occupied frontier levels are very much

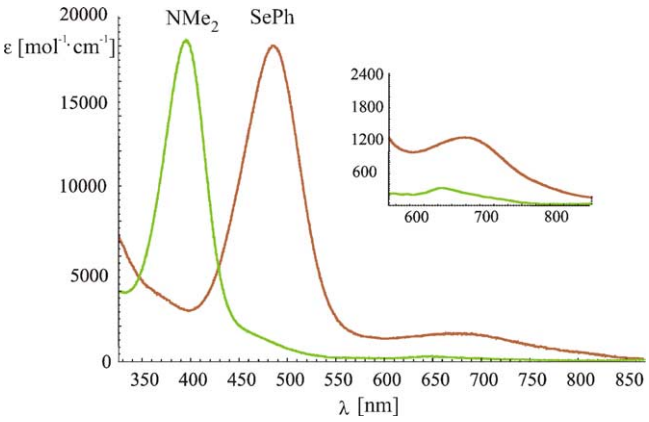

Fig. 2. Optical absorption spectra of the allenylidene complexes *trans*-$[Cl(dppm)_2Ru{=}C{=}C{=}C(ER_n)(C_4H_7)]^+$ in CH_2Cl_2 (insert: HOMO → LUMO band magnified).

concentrated on the {ClRu} entity, which contributes about 80% of the total electron density. The LUMO, on the other hand, is delocalized over the allenylidene ligand with only minor contributions of the metal and the chloride ligand. A graphical display of the crucial frontier orbitals of the *trans*-$[Cl(PH_3)_4Ru{=}C{=}C{=}C\{(N(CH_3)_2\}(CH_3)]^+$ model complex is given as Fig. 3 and may serve to illustrate this point. Both transitions thus involve a fair amount of charge

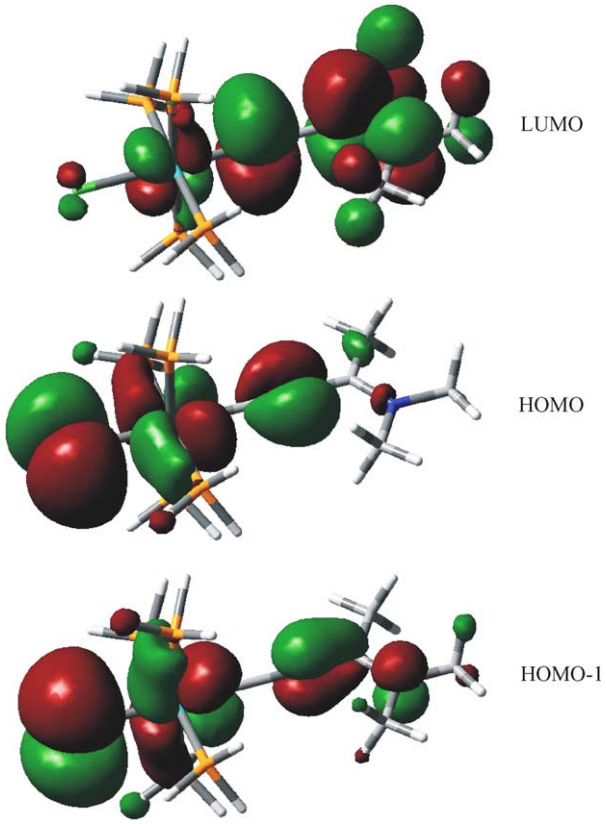

Fig. 3. Graphical representations of the frontier orbitals of *trans*-$[Cl(PH_3)_4Ru{=}C{=}C{=}C\{N(CH_3)_2\}(CH_3)]^+$.

Table 4
Experimentally determined absorption energies for allenylidene complexes *trans*-[Cl(dppm)$_2$Ru=C=C=C(ER$_n$)(R′)]$^+$

Band	ER$_n$/R′ N(CH$_3$)$_2$/CH$_3$	ER$_n$/R′ SMe/C$_4$H$_7$	ER$_n$/R′ SeC$_3$H$_5$/C$_4$H$_7$	ER$_n$/R′ Me/Me	ER$_n$/R′ Ph/Ph
HOMO → LUMO (eV)	1.93	1.78	1.82	1.71	1.50
HOMO-1 → LUMO (eV)	3.17	2.61	2.53	2.99	2.43

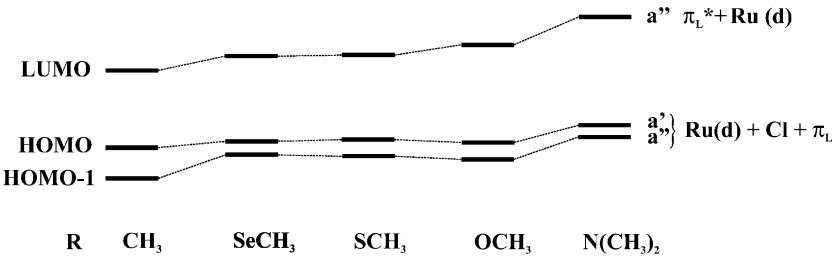

Fig. 4. Relative energies of the DFT calculated frontier levels for differently substituted allenylidene complexes *trans*-[Cl(PH$_3$)$_4$Ru=C=C=C(ER$_n$)(CH$_3$)]$^+$.

transfer from the {ClRu} entity to the organic acceptor ligand despite an only small negative solvatochromism of ca 600 cm^{-1} for the HOMO-1 → LUMO and 75–200 cm^{-1} for the HOMO → LUMO bands for solutions in CH_2Cl_2 and CH_3CN. Experimental evidence for the character of these bands comes from Resonance Raman spectroscopy on alkylthio and aryl substituted complexes. In this technique, only those vibrational modes that are directly influenced by the corresponding electronic transition are resonantly enhanced [102]. In every instance there are prominent Raman bands arising from the C=C=C stretch and the Ru–Cl stretch near 320 cm^{-1} [103].

Absorption energies for complexes *trans*-[Cl(dppm)$_2$Ru=C=C=C(ER$_n$)(R′)]$^+$ are collected in Table 4. A decreasing donor ability of the ER$_n$ group induces a bathochromic shift of both absorption bands. Our DFT calculations and electrochemical measurements (vide infa) agree in attributing this systematic trend to a preferential lowering of the LUMO orbital within the series N(CH$_3$)$_2$ > OCH$_3$ > SCH$_3$ ≈ SeCH$_3$ > Me > Ph. Fig. 4 displays the relative energies of the crucial frontier orbitals as a function of the ER$_n$ substituent while the energies and compositions of these orbitals are provided in Table 5. It is worth noting that the calculated energies reproduce the peculiar optical properties of the dimethyl substituted complex *trans*-[Cl(dppm)$_2$Ru=C=C=C(CH$_3$)$_2$]$^+$. This species exhibits a red-shift of the HOMO → LUMO band when compared to the SeR and SR substituted congeners but a HOMO-1 → LUMO band in the same energy range as is observed for amino substituted derivatives. This points to a rather large energy gap between the HOMO and the HOMO-1 levels in good agreement with the calculated orbital energies.

A property which is unique for the amino substituted complexes is the presence of another weak band appearing as a

Table 5
Calculated electron energies and compositions of the frontier orbitals for model complexes *trans*-[Cl(PH$_3$)$_4$RuC$_3${E(CH$_3$)$_n$}(CH$_3$)]$^+$ (per cent contributions according to Mulliken population analysis)

E(CH$_3$)$_n$	MO	*E* (eV)	Dominating character[a]	Ru	C$_1$	C$_2$	C$_3$	E	Cl
N(CH$_3$)$_2$	LUMO	−5.90	π* (ER$_n$) + d$_{Ru}$	10(d)	27	2	34	18	1
	HOMO	−7.85	Ru + Cl + π* (ER$_n$)	35(d)	1	14	1	0	44
	HOMO-1	−8.06	Ru + Cl + (PH$_3$)$_4$	23(d)	0	6	2	5	57
O(CH$_3$)	LUMO	−6.38	π* (ER$_n$) + d$_{Ru}$	12(d)	29	2	37	14	2
	HOMO	−8.15	Ru + Cl + π* (ER$_n$)	36(d)	2	16	1	1	41
	HOMO-1	−8.46	Ru + Cl + (PH$_3$)$_4$	19(d)	0	5	4	5	62
S(CH$_3$)	LUMO	−6.57	π* (ER$_n$) + d$_{Ru}$	12(d)	25	3	36	18	2
	HOMO	−8.12	Ru + Cl + π* (ER$_n$)	37(d)	2	16	1	1	37
	HOMO-1	−8.40	Ru + Cl + (PH$_3$)$_4$	21(d)	0	6	3	12	54
Se(CH$_3$)	LUMO	−6.59	π* (ER$_n$) + d$_{Ru}$	13(d)	26	3	35	17	2
	HOMO	−8.13	Ru + Cl + π* (ER$_n$)	38(d)	3	17	–	2	35
	HOMO-1	−8.41	Ru + Cl + (PH$_3$)$_4$	20(d)	0	7	2	20	46
CH$_3$	LUMO	−6.85	π* (ER$_n$) + d$_{Ru}$	15(d)	31	2	36	7	2
	HOMO	−8.26	Ru + Cl + π* (ER$_n$)	37(d)	5	19	1	2	32
	HOMO-1	−8.80	Ru + Cl + (PH$_3$)$_4$	15(d)	2	2	5	1	69

[a] π* (ER$_n$) denotes an antibonding π orbital of the C=C=C(ER$_n$)(R′) ligand.

shoulder on the low energy side of the intense HOMO-1 → LUMO absorption. Based on the results of time-dependent (TD) DFT calculations, this feature has been attributed to the spin-forbidden singlet-to-triplet (S → T) HOMO-1 → LUMO transition. Population of the excited triplet state is thus quite efficient for these systems. Since thermal deactivation to the lowest triplet state is slow, this leads to the rather unusual observation of a long-lived emission from an excited triplet state with a half-life of up to 175 μs at 77 K. Irradiation into the HOMO → LUMO band gives rise to another emission at considerably lower energies, this time from the lowest triplet state [103].

Optical spectra of the aryl substituted allenylidene derivatives *trans*-[Cl(dppm)$_2$Ru=C=C=C(Ph)(R)]$^+$ display additional bands at 391 and 320 nm (R = Me) or 412, 355 and 339 nm (R = Ph). Similar, but significantly more intense absorptions are also observed for aryl substituted carbocations as is exemplified by PhMe$_2$C$^+$ (λ_{max} = 390 and 326 nm) and Ph$_2$MeC$^+$ (λ_{max} = 422 and 312 nm) [104]. This close correspondence may be another indication for the retaining of some alkynyl character within the allenylidene ligand. Some fraction of the positive charge would then remain on the terminal C$_\gamma$(Ph)(R) moiety as is expressed by the resonance froms **III** and **IV** in Plate 1.

3.4. ^{13}C NMR spectroscopy

Besides the IR and optical properties, the substituents attached to carbon atom C$_\gamma$ also have a strong bearing on the ^{13}C NMR spectra of the allenylidene complexes. Assignment of the resonance signals to individual positions along the carbon chain rests on the P–C coupling constants which are thought to continuously diminish with increasing spatial separation ($^2J_{P-C} \approx 14$ Hz, $^3J_{P-C} \approx 1.9$ Hz, $^4J_{P-C} \approx 1.1$ Hz) [27]. In the case of complexes *trans*-[Cl(dppm)$_2$Ru=C=C=C(Aryl)(H)]$^+$ containing secondary allenylidene ligands, the sequence $\delta(C_\alpha) > \delta(C_\beta) > \delta(C_\gamma)$ was unambiguously established by virtue of the $^nJ_{C-H}$ coupling constants and was found to match that derived from the $^nJ_{P-C}$ pattern [72]. Moreover, the order $\delta(C_\alpha) > \delta(C_\gamma) > \delta(C_\beta)$ derived for amino substituted allenylidene ruthenium complexes based on P-C coupling constants [11,27,34] fully agrees with that derived for similar neutral complexes of pentacarbonyl tungsten based on the $^nJ_{W-C}$ couplings [16,17]. Table 6 lists the characteristic shift ranges for individual carbon atoms along the unsaturated ligand for differently substituted derivatives *trans*-[Cl(dppm)$_2$Ru=C=C=C(ER$_n$)(R′)]$^+$ and compares them to calculated values for the PH$_3$ substituted models. We note a good overall agreement between the experimental and calculated values. Even though individual values may be off by some 10–30 ppm, the trends are correctly reproduced.

The experimental data reveal a somewhat paradoxical behaviour: the closer the carbon atom is to the actual substitution site, the lesser its chemical shift is influenced by the identity of the ER$_n$ moiety. Thus, the chemical shifts for the metal bonded C$_\alpha$ cover a range of about 100 ppm when comparing amino and aryl or alkyl substituted congeners, which again occupy diametral positions within this series. The shift range for the internal carbon atom C$_\beta$ is somewhat smaller (about 80 ppm), whereas the resonance signals for C$_\gamma$ are within a range of just 30 ppm. The same observations hold for Touchard's arene half-sandwich complexes [(η^6-C$_6$Me$_6$)(L)ClRu=C=C=C(ER$_n$)(CH=CPh$_2$)]$^+$ (L = PMe$_3$, PMe$_2$Ph, ER$_n$ = NR$_2$, OR, aryl) [12–15] and Tamm's allenylidene complexes [Cp(PPh$_3$)$_2$Ru=C=C=C(cht^R)]$^+$ having substituted cycloheptatrienyl substituents [71]. This is in sharp contrast to organic allenes, where substitution mainly effects the ^{13}C resonance shift at the actual substitution site [67,105].

Table 6
Experimental and calculated ^{13}C NMR shifts for the carbon atoms of the allenylidene ligand in *trans*-[Cl(dppm)$_2$Ru=C=C=C(ER$_n$)(R′)]$^+$

	ER$_n$	$\delta(C_\alpha)$ (ppm)	$\delta(C_\beta)$ (ppm)	$\delta(C_\gamma)$ (ppm)
Experimental	NR$_2$	202–213	119–125	152–157
	OR[a]	253	150	156
	SR	283–286	170–172	168–171
	SeR	297–305	180–185	169–181
	Alkyl/Aryl	310–325	200–205	163–173
Calculated[b]	N(CH$_3$)$_2$	224	111	138
	OCH$_3$	242	125	146
	SCH$_3$	273	145	165
	SeCH$_3$	289	150	183
	CH$_3$	318	172	179

[a] For *trans*-[Cl(dppm)$_2$Ru=C=C=C(OMe)(CH=CPh$_2$)]$^+$ according to ref. [15].
[b] Calculated values for R′ = Me.

The in part extreme low-field shifts of these signals are dominated by the paramagnetic shift term which in turn depends on the wave functions of the ground and the excited states, such that spatially remote atoms may significantly contribute to the shift of an individual nucleus. Moreover, the paramagnetic shift contribution is inversely proportional to the energy gap between the occupied and empty frontier levels [106]. There is indeed a close correspondence between the shift of the allenylidene carbon atoms and the energies of the HOMO → LUMO and the HOMO-1 → LUMO transition energies derived from optical spectroscopy, and we will come back to this point in a later section.

All carbon substituted allenylidene complexes may well be compared to related carbocations R^{1}C≡C–C$^+$R^{2}R^3 (R^1, R^2, R^3 = Ph, Me). In these latter systems, a shift of the resonance signals for the outer carbon atoms to lower field is taken as evidence for a higher contribution of the cumulenic resonance form R^{1}C$^+$=C=CR^{2}R^3 [107–110]. A comparison of the data for allenylidene complexes *trans*-[Cl(dppm)$_2$Ru=C=C=C(R)(R′)]$^+$ (R = Ph, R′ = Me, Ph or R = R′ = Me) to their fully organic counterparts indicates a drastic deshielding for carbon atoms C$_\alpha$ and C$_\beta$ and a concomitant shielding of C$_\gamma$. This indicates a dominant contribution of the cumulenic resonance form for

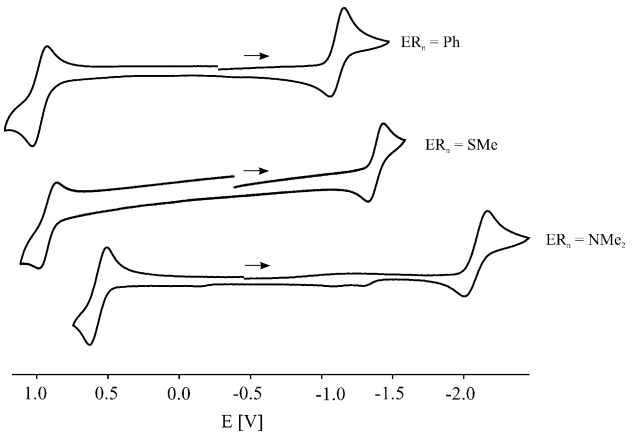

Fig. 5. Cyclic voltammograms of complexes *trans*-[Cl(dppm)$_2$Ru=C=C=C(ER$_n$)(alkyl)]$^+$ in CH_2Cl_2/NBu_4PF_6; ER$_n$ = Ph, SMe: v = 0.1 V/s, T = 298 K, ER$_n$ = NMe$_2$: v = 1.0 V/s, T = 195 K.

aryl substituted allenylidene complexes whereas the corresponding carbocations are much better represented by their propargylic resonance forms.

3.5. Electrochemical investigations

Electrochemically determined half-wave potentials provide an alternative source of information on the energies of the frontier orbitals. Here, one assumes that reduction potentials reflect the LUMO energies and oxidation potentials those of the HOMO orbitals. Such reasoning, however, requires that the sequence of the frontier orbitals remains unaltered upon the electron transfer process and assumes the validity of Koopmann's theorem. This is not always justified and there is a growing number of instances, where Koopmann's theorem has been recognized to be a rather poor approximation in transition metal chemistry [111,112]. Any meaningful discussion requires thermodynamically defined half-wave potentials and this in turn necessitates, that the electrochemical processes under study are chemically and electrochemically reversible, at least on the time-scale of the electrochemical experiment.

With the exception of the dimethyl substituted derivative *trans*-[Cl(dppm)$_2$Ru=C=C=C(CH$_3$)$_2$]$^+$, all of our allenylidene complexes comply to these requirements, even though it was sometimes necessary to resort to low temperatures down to −78 °C and higher sweep rates in order to slow chemical follow steps to a degree that allowed us to observe an associated counter peak in cyclic voltammetry experiments [11,32,34]. The voltammetric traces of some representative complexes that differ in just the ER$_n$ substituent are compared in Fig. 5, while typical ranges of redox potentials for each ER$_n$ group are given in Table 7.

All of the complexes under study display two more or less reversible features: An anodic oxidation and a cathodic reduction. As the NR$_2$ moiety is replaced by SR, SeR or aryl groups, there is a continuous anodic shift of the half-wave potentials of both these processes. From the data in Table 7 it

Table 7
Redox potentials for differently substituted allenylidene complexes *trans*-[Cl(dppm)$_2$Ru=C=C=C(ER$_n$)(R′)]$^+$ (data in CH_2Cl_2/NBu_4PF_6)

ER$_n$	R′	$E^{ox}_{1/2}$ (V)	$E^{red}_{1/2}$ (V)
NMe$_2$	Alkyl	+0.57 to +0.64	−2.09 to −2.18
SR	Alkyl	+0.85 to +0.89	−1.36 to −1.38
SeR	Alkyl	+0.89 to +0.93	−1.34 to −1.36
1-Methylpyrrol-2-yl	CH_3	+0.66	−1.33
Ph	Me	+0.96	−1.13
Ph	Ph	+0.99	−1.035, −2.14

is immediately apparent, that the ER$_n$ moiety influences the reduction potential much stronger than that of the oxidation. These alterations mirror the energy changes of the frontier orbitals upon substitution (see Fig. 4) and fully agree with the above reasoning.

3.6. Spectroscopic and electrochemical data in correlation

Knowing the oxidation and the reduction potentials gives direct access to the energy difference $\Delta E_{el} = E^{ox}_{1/2} - E^{red}_{1/2}$ as an approximate measure for the energy difference between the frontier orbitals. Since similar information is available from optical spectroscopy, one would expect to see a close correspondence between the optically and the electrochemically derived energy gaps.[2] We indeed observe a good linear correlation between the two data sets. Thus, R^2 values of 0.95 are obtained, when the HOMO-1 → LUMO or the HOMO → LUMO transition energies are plotted against ΔE_{el} (see Supplementary Materials of the supporting information). As has been mentioned before, the energy difference of the frontier orbitals and the ^{13}C NMR shifts of the carbon atoms of the unsaturated ligand should be directly related via the paramagnetic shift term, assuming that other influences like the p-character of the relevant orbitals and their symmetry properties remain constant within this series of complexes. In fact, close linear relations are obtained for C_α and C_β (R^2 ca. 0.96), when the ^{13}C NMR parameters are plotted against ΔE_{el} or the energies of the optical transitions. Owing to the small sensitivity of the chemical shift of the carbon atom C_γ to the nature of the attached substituent, poorer correlations are observed for this carbon atom. The correlation to the absorption energies of the HOMO-1 → LUMO transition, as is exemplified by Fig. 6, illustrates this point. Plots for the other parameters are provided as Supplementary Materials.

We have already discussed that a bathochromic shift of the optical absorption bands, and, likewise, a lower splitting of the redox potentials, parallels an increasing cumulenic character of the allenylidene ligand. One would therefore also expect to see a correlation between any of these parameters

[2] Of course, standard potentials derived from electroanalytical solution experiments give energy differences between oxidized and reduced forms, such that other effects like changes in solvation energies or electrostatic effects from ion pairing also play an important role.

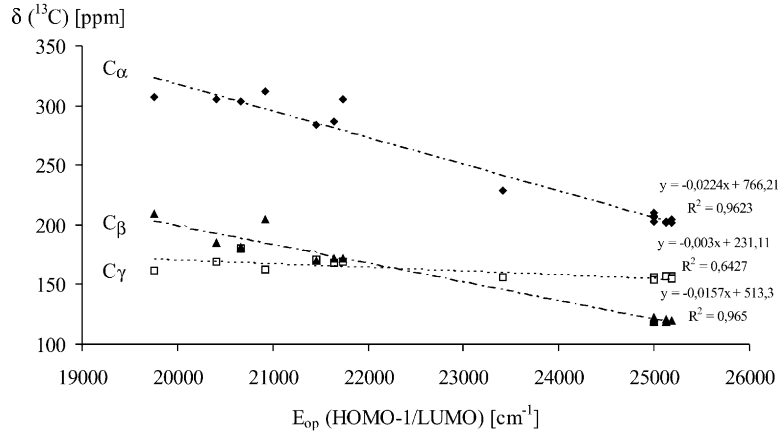

Fig. 6. Correlation between the ^{13}C NMR shifts for the carbon atoms of the allenylidene ligand and the energy of the optical HOMO-1 → LUMO transition.

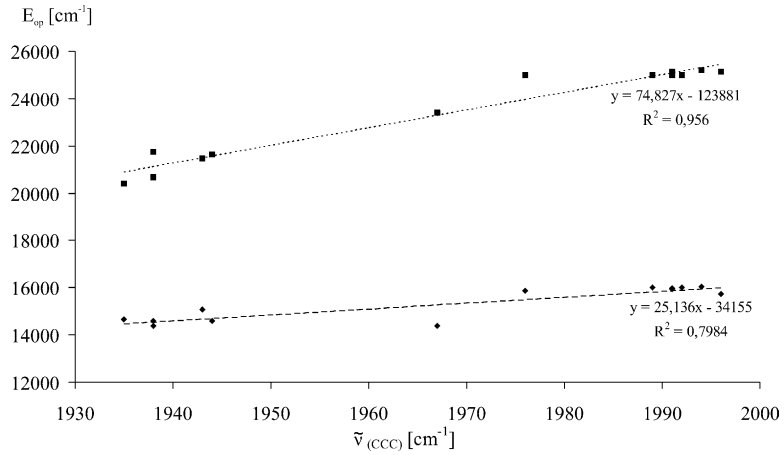

Fig. 7. Plot of optical transition energies versus the frequency of the CCC stretch of the allenylidene ligand. Upper trace: HOMO-1 → LUMO transition, lower trace: HOMO → LUMO transition.

and the energy of the CCC valence stretch. This is indeed the case. Thus, plots of ΔE_{el}, E_{op} (HOMO-1 → LUMO), E_{op} (HOMO → LUMO), and of $\delta(^{13}C)$ parameters against the energy of the CCC stretch give good linear correlations in most cases. Fig. 7 provides one such example while other correlations are provided in the Supporting Material (Supplementary Materials).

The important implication of such correlations is, that each of the electrochemical or spectroscopic parameters may be taken by itself as a manifestation of the bonding within these systems, i.e. for the assessment of the alkynyl versus the cumulenic character. We are therefore able to give reliable estimates for any of these parameters for any $\{Cl(dppm)_2Ru\}$ derived allenylidene complex, if only one of them has been experimentally determined. This is an essential for a rational fine-tuning of any property of such allenylidene complexes, e.g. generating a complex with an optical absorption in a specific energy range. It is quite evident, that similar correlations should exist for any other families of differently substituted allenylidene complexes derived from a certain metal entity $\{L_nM\}$ and we anticipate to see more of those, as other series of allenylidene complexes with a wider spectrum of different substituents attached to the allenylidene ligand and different metal/ligand combinations are investigated.

3.7. The influence of the metal entity

As is expected of a highly delocalized organometallic π-system, the metal entity should also imprint its mark on the properties of the allenylidene complexes. For monocationic complexes, a higher electron density at the metal should lead to a higher contribution of the cumulenic resonance form, where the positive charge resides at the metal. An experimental verification is provided by the series of the dimethylallylamine derived complexes *trans*-$[Cl(L_2)_2Ru{=}C{=}C{=}C(NMe_2)(C_4H_7)]^+$ where L_2 is 1,2-$Ph_2PC_2H_4PPh_2$ (dppe), $Ph_2PCH_2PPh_2$ (dppm) or $Et_2PC_2H_4PEt_2$ (depe) [113].[3] The systematic trends within

[3] Despite having identical substituents, the dppm and dppe ligands differ by enforcing substantially different PRuP angles at the metal. This renders the dppm ligand seemingly more electron rich than the dppe ligand.

this series of complexes fully adhere to these assumptions. We thus find a pronounced bathochromic shift of the $\tilde{\nu}_{CCC}$ and HOMO-1 → LUMO band as well as a low-field shift of $\delta(C_\alpha)$ as the electron density at the metal increases in the order dppe < dppm < depe [11]. A notable exception is the insensitivity of the shift of carbon atom C_β to the diphosphine co-ligands. This probably arises from the fact that carbon atom C_β has only negligible contributions to the metal dominated occupied frontier levels. Another interesting observation is, that the oxidation potentials of these complexes strongly depend on the identity of the ligand L_2 while the reduction potentials remain identical across this series. We view this as another indication of the small contribution of the metal to the LUMO orbital.

Substitution of the $\{ClRu(L_2)_2\}$ entity by another, more electron rich one therefore has the same overall effect as exchanging the substituent at carbon atom C_γ by a weaker electron donor. This further underlines the pronounced push–pull characteristics of these complexes and highlights the aspect of electronic interactions across the unsaturated ligand.

3.8. Allenylidene complexes having electroactive substituents and ligands

The attachment of electroactive substituents or ligands to the metallabutatriene chromophore provides an alternative to influencing the bonding in allenylidene complexes other than substituting the ER_n moiety at carbon atom C_γ or replacing the diphosphine ligands. Such modification allows to probe for the effect of varying the electron density at each of these sites within the same basic system without the need for further substitution. The construction of such systems requires that these secondary electroactive groups are reversibly oxidized (reduced) at less anodic (cathodic) potentials than the parent allenylidene complexes themselves. Given their essentially Nernstian redox-behaviour, ferrocene derivatives ideally suit that purpose. Moreover, the rich chemistry of ferrocenes offers many opportunities to attach them to any specific position within the metallabutatriene chromophore and thus to probe, how electronic ligand or substituent effects are propagated across the entire system. Ferrocenyl containing allenylidene complexes such as $[(\eta^6\text{-}C_6Me_6)Cl(PMe_3)Ru{=}C{=}C{=}C(Ph)(Fc)]^+$ [53] and $[Tp(dppf)Ru{=}C{=}C{=}CPh_2]^+$ [93] had been reported before, but none of these studies utilized their potential as to visualizing the spectroscopic changes brought about by ferrocene oxidation. In order to monitor the spectroscopic changes concomitant with oxidation of these secondary redox tags, we have utilized spectroelectrochemical techniques. In this approach, the species of interest is generated inside a thin-layer electrolysis cell as was described by Hartl and co-workers [114]. Spectra are recorded while the potential is held at an appropriate value or while very slowly scanning the respective voltammetric wave.

A first complex with this general design is *trans*-$[Cl(dppm)_2Ru{=}C{=}C{=}C(NMe_2)(C_2H_4Fc)]^+$ (Fc = $(\eta^5\text{-}C_5H_4)Fe(\eta^5\text{-}C_5H_5)$), which was formed upon trapping *trans*-$[Cl(dppm)_2Ru{=}C{=}C{=}CH_2]^+$ with (dimethylaminomethyl) ferrocene (Scheme 3). Oxidation of the ferrocenyl moiety caused a slight red-shift of the intense charge transfer band in the visible region. A shift of the allenylidene IR band was, however, not observed and thus amounts to no more than some 2–3 wavenumbers [31]. Given the large spatial separation between the terminal carbon atom of the allenylidene ligand and the ferrocenyl entity and the insulating character of the ethylene spacer, this result was not unexpected. In *trans*-$[Cl(dppm)_2Ru{=}C{=}C{=}C(SeFc)(C_2H_4CH{=}CH_2)]^+$, the redox active ferrocenyl substituent is directly attached to the allenylidene ligand. Oxidation of the ferrocenylselenyl group causes a red shift of the allenylidene IR band by $10\,cm^{-1}$ [35]. This is in full agreement with what one would expect of the replacement of a substituent ER_n by a weaker donor.

The next step was then to link a ferrocenyl substituent directly to the terminal carbon atom of the allenylidene ligand. Our efforts along these lines have so far not been successful within the *trans*-$\{Cl(L_2)_2Ru\}$ series. It was, however, easily accomplished for $\{TpL_2Ru\}$ based complexes containing the hydridotris(pyrazolyl)borate (Tp) ligand [61,93], following the now-classical Selegue route [51]. These complexes offer the additional advantage of allowing for the introduction of a redox active dppf (dppf = 1,1'-bis(diphenylphosphino)ferrocene) ligand and thus to probe for the effect of decreasing the electron density at the metal. We have prepared and studied all of the three possible combinations of ferrocene containing complexes $[TpL_2Ru{=}C{=}C{=}C(Ph)(R)]^+$ (R = Fc, L_2 = 2 PPh_3, dppf; R = Ph, L_2 = dppf) with either a ferrocenyl substituent attached to the terminal carbon atom of the allenylidene ligand or the redox active dppf-chelate bonded to the metal or both [115].

As the ferrocenyl substituent in $[Tp(PPh_3)_2Ru{=}C{=}C{=}C(Ph)(Fc)]^+$ is oxidized, the allenylidene band shifts by $20\,cm^{-1}$ to lower energy (Fig. 8a). This shift is twice that observed for the ferrocenylselenyl substituted complex discussed above and shows, how the magnitude of this effect increases with conjugation within the chromophore. In $[Tp(dppf)Ru{=}C{=}C{=}CPh_2]^+$, oxidation of the dppf ligand has the opposite effect of inducing an average shift of the allenylidene ligand by $15\,cm^{-1}$ to higher energy (Fig. 8b). The most likely explanation for the splitting of the original single band into two neighbouring absorptions is a Fermi-type coupling, possibly with a =C–C(Ph) mode. IR spectroelectrochemistry provided us also with a means to assign the two closely spaced redox waves observed in the potential range typical of ferrocene based redox processes for $[Tp(dppf)Ru{=}C{=}C{=}C(Ph)(Fc)]^+$ to the individual redox events. Upon the first oxidation, there is a red shift of the allenylidene band by $20\,cm^{-1}$ accompanied by some distinct loss of molar absorptivity as is only compatible with the oxidation of the allenylidene bound ferrocenyl substituent. The second oxidation, now at the dppf site, has exactly the

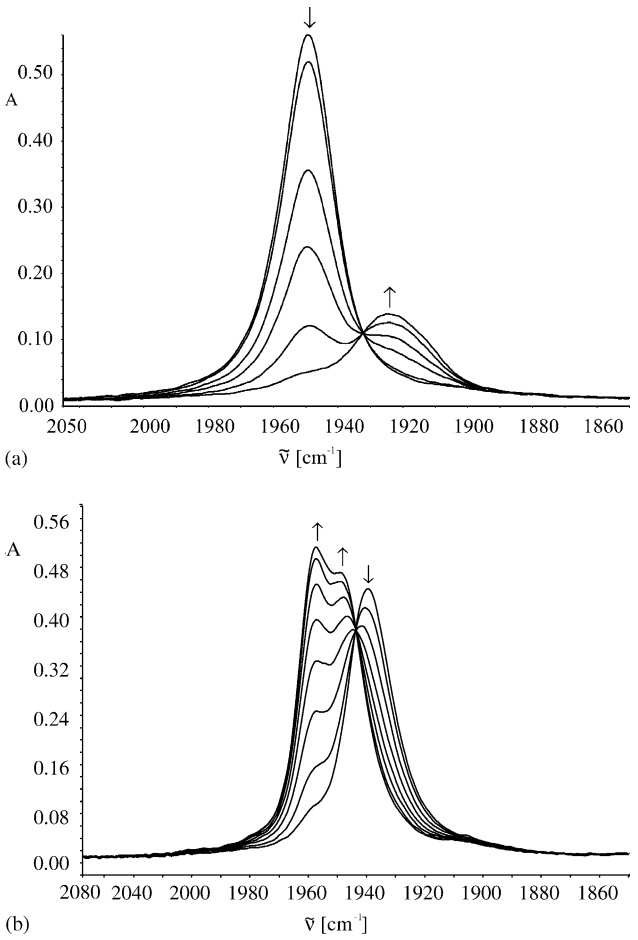

Fig. 8. (a). IR-Spectroscopic changes upon oxidation of the ferrocenyl substituent in $[Tp(PPh_3)_2Ru{=}C{=}C{=}C(Fc)(Ph)]^+$ (Tp = tris(pyrazolyl)borate, Fc = ferrocenyl). (b) IR-Spectroscopic changes upon oxidation of the dppf-ligand in $[Tp(dppf)Ru{=}C{=}C{=}CPh_2]^+$ (Tp = tris(pyrazolyl)borate, dppf = 1,1'-bis(diphenylphosphino)ferrocene).

opposite effect and shifts the allenylidene band back to its original position in the starting monocation. The relative intensity changes, i.e. an intensity decrease upon decreasing the electron density at the allenylidene ligand but an intensity increase upon reducing the electron density at the metal has been interpreted as arising from the differences in dipole moment change during the underlying C=C=C vibration. In the monocationic starting compounds, the positive charge largely resides on the $\{Tp(L_2)Ru\}$ entity. As the electron density at this site further diminishes, the CCC stretch leads to an even larger charge separation and hence a more intense IR absorption. The opposite is true, when ferrocenyl oxidation at the C terminus of the allenylidene complex generates another positive charge at the opposite end of the metallabutatriene chromophore.

The sequence of redox events in $[Tp(dppf)Ru{=}C{=}C{=}C(Ph)(Fc)]^+$ was also confirmed by a combination of electrolysis and optical spectroscopy. In contrast to their all phenyl substituted counterparts, the ferrocenyl phenyl substituted complexes $[Tp(L_2)Ru{=}C{=}C{=}C(Ph)(Fc)]^+$ exhibit

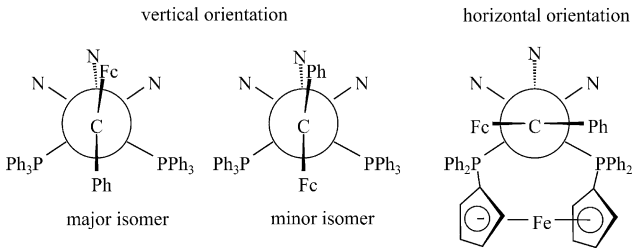

Plate 5.

a highly intense ferrocenyl-to-allenylidene charge transfer band peaking at 710–720 nm. This band bleaches out when the ferrocenyl substituent is oxidized. It was found, that this happens during the first oxidation of $[Tp(dppf)Ru{=}C{=}C{=}C(Ph)(Fc)]^+$ in complete agreement with the results from IR-spectroelectrochemistry.

As an interesting observation at the side, we have found, that the unsymmetrically substituted complexes $[TpL_2Ru{=}C{=}C{=}C(Ph)(Fc)]^+$ provide the first examples of allenylidene complexes that display a hindered rotation of the allenylidene ligand around the Ru=C bond. $[Tp(PPh_3)_2Ru{=}C{=}C{=}C(Ph)(Fc)]^+$ exists as a mixture of two isomers in a 4:1 ratio. Each isomer gives rise to a sharp singlet in the ^{31}P NMR spectrum which is indicative of a vertical alignment of the allenylidene plane where the CRR′ unit is parallel to the complex cation's molecular mirror plane. These isomers differ in which substituent, phenyl or ferrocenyl, points towards the Tp and the PPh_3 ligands (Plate 5). Up to 388 K where the compound started to decompose, no signs of coalescence were observed such that the energy barrier to rotation of the allenylidene ligand around the Ru=C bond must be quite substantial. The dppf substituted congener displays just one singlet in its room temperature ^{31}P NMR spectrum. Upon cooling, this signal splits into a well-resolved AB quartet. This points to a horizontal alignment of the allenylidene ligand in the ground state, possibly because of a steric hindrance between the allenylidene substituents and the dppf backbone (Plate 5). At the coalescence temperature of 238 K, the energy barrier amounts to 47 kJ/mol and is thus significantly lower as in the PPh_3 substituted congener. A possible explanation takes into account the different orientations of the allenylidene ligand in these two complexes. As it has been noted before, the vertical orientation is the lower energy minimum with respect to the horizontal one [116,117]. In $[Tp(dppf)Ru{=}C{=}C{=}C(Ph)(Fc)]^+$ this orientation can not be achieved such that allenylidene rotation involves an energetically less favourable ground state structure and hence a lower energy barrier.

4. Summary and conclusions

Cumulenylidene complexes $[\{Ru\}{=}C_n{=}CRR']^+$ having an extended unsaturated ligand are easily transformed into

a wide variety of allenylidene complexes [{Ru}=C=C=C(ER_n)(R′)]$^+$ {Ru} = CpRu(PPh_3)$_2$, *trans*-{Cl(dppm)$_2$Ru}, {(η^6-arene)RuCl(PR_3)}). The two principle synthetical pathways are the regioselective nucleophilic addition of protic nucleophiles to the C_γ=C_δ bond (n = 3, 4) and a reaction sequence involving the nucleophilic addition of aprotic, allyl or propargyl substituted nucleophiles to carbon atom C_γ followed by Cope-type rearrangement within the 3-heteroatom substituted hexa-1,5-diene subunit of the primary addition product. These methods add to the powerful, now classical Selegue route. Taken together, they allow the ER_n moiety to be varied from NR_2, OR, SR, SeR to alkyl, aryl or pyrrolyl groups. In depth spectroscopic and electrochemical investigations were carried out on a series of complexes of the *trans*-{Cl(L_2)$_2$Ru} entity. They reveal, how the electronic properties of the ER_n moiety alter the bonding in these complexes along a continuum spanning the genuine cumulenic and alkynyl type structures. The alkynyl character becomes more and more prevalent as the donor capacity of the ER_n group increases. This is accompanied by a blue shift of the CCC stretch in the IR and the optical absorption bands in the visible regime. In ^{13}C NMR spectroscopy, the resonances of the allenylidene carbon atoms are progressively shifted to higher field. Carbon atoms C_α and C_β provide the most sensitive probe. Curiously enough, the effect on the shift of carbon atom C_γ, which constitutes the actual substitution site, is only small. Comparison with purely organic cumulenes shows that substituent effects are strongly attenuated upon metal binding. Specifically, aryl substituted allenylidene ligands are much more cumulenic and amino substituted ones much more "propargylic" than their purely organic counterparts. The data presented herein make clear, that the different spectroscopies provide a much more detailed picture of the bonding in allenylidene complexes than is available from X-ray crystallography. Individual CC bonds within the allenylidene ligand are rather insensitive to the ER_n substituent such that subtle changes are mostly disguised by the inherently low experimental precision of the diffraction experiment.

Electrochemical investigations have shown that these allenylidene complexes may be oxidized and reduced by one electron each. Substitution at the terminal carbon atom alters the oxidation and the reduction potentials with much larger effects on the latter. In contrast substitution of the diphosphine ligands affects only the oxidation potential while leaving the reduction potential unchanged. This points to a largely metal-based oxidation and a dominantly ligand-centered reduction, and there is growing experimental evidence to support this view [5,11,32,34,65]. Allenylidene complexes having electroactive ligands or substituents have also been studied. They serve as single molecule probes for the conclusions derived from the body of differently substituted allenylidene complexes and demonstrate the strong push-pull characteristics of these organometallic cumulenes.

Quantum mechanical investigations on model complexes with PH_3 or $H_2PCH_2PH_2$ as co-ligands have not only confirmed the experimental findings but also added considerably to our understanding of the bonding within these systems. Of special relevance is, that the CCC stretch has been identified as to almost exclusively involve the $C_\alpha C_\beta$ bond, and this provides a rational for correlating its energy to the character of this specific bond. They have also shown, that the energy barrier to rotation around the C_γ=NR_2 bond in amino substituted allenylidene complexes represents a genuine electronic and not a steric effect. In addition, they revealed the strong metal-to-ligand charge transfer character of the optical transitions despite their only weak solvatochromism and helped to rationalize their grossly different intensities. Based on calculations, the red shift of these transitions upon replacement of an NR_2 by a SR, SeR, alkyl or aryl substituent has been traced to a preferential lowering of the LUMO orbital. This matches the observed trends in redox potentials.

Close correlations between any pair of electrochemical or spectroscopic parameters demonstrate, that every single one of them provides a measure of the bonding within these complexes and may now be used independently in its assessment. Similar correlations should exist for any other series of differently substituted allenylidene complexes comprising different metal/ligand combinations.

5. DFT calculations

Ground state electronic structure calculations have been performed by density-functional theory (DFT) methods using Amsterdam Density Functional (ADF2002.3) [118,119] and Gaussian 98 [120] program packages. Within Gaussian 98 Dunning's valence double-ξ functions [121] with polarization functions were used for H, C, N and Cl atoms and the effective quasirelativistic effective core pseudopotentials and corresponding optimized set of basis functions for P [122] and Ru [123] atoms. Hybrid Becke's three parameter functional with Lee, Yang and Parr correlation functional (B3LYP) [124] was used in Gaussian 98 calculations (G98/B3LYP). Within the ADF program Slater type orbital (STO) the following basis sets were used: double-ξ quality for H atoms, triple-ξ quality with polarization functions for H, C, N, P, Cl and Ru. Inner shells were treated within the frozen-core approximation (1s for C and N, 1s–2p for P and Cl, 1s–3d for Ru). Local density approximation (LDA) with VWN parametrization of electron gas data including Becke's gradient correction [125] to the local exchange expression in conjunction with Perdew's gradient correction [126] to the LDA correlation was used (ADF/BP). The scalar relativistic (SR) zero order regular approximation (ZORA) was used. Tabulated structural parameters, molecular orbital diagrams and the orbital analysis were based on the ADF/BP calculations. Frequencies and NMR isotropic shifts were calculated by G98/B3LYP at structures optimised using the same functional and basis set.

Acknowledgements

R.F.W. is indebted to the Fonds der Chemischen Industrie, Deutsche Forschungsgemeinschaft and to VW-Stiftung for the financial support of this research. He also thanks his co-workers Ralf-Christoph Harbort and Stephan Hartmann for their enthusiastic and competent work and those undergraduate students who have contributed to these results. S.Z. thanks the Ministry of Education of the Czech Republic, COST (grant number OC D14.20) and the Grant Agency of the Czech Republic, grant No. 203/03/082. The author's collaboration was financed by VW-Stiftung. Johnsson & Matthey is acknowledged for a loan of $RuCl_3$.

References

[1] E.O. Fischer, Pure Appl. Chem. 24 (1970) 407.
[2] E.O. Fischer, M. Leupold, C.G. Kreiter, J. Müller, Chem. Ber. 105 (1972) 150.
[3] E.O. Fischer, G. Kreis, F.R. Kreißl, C.G. Kreiter, J. Müller, Chem. Ber. 106 (1973) 3910.
[4] E.-O. Fischer, H.J. Kalder, A. Frank, F.H. Köhler, G. Huttner, Angew. Chem. 88 (1976) 683.
[5] R.F. Winter, Rutheniumkomplexe mit hoch ungesättigten C_3- und C_4-Liganden aus Diacetylen, Verlag Grauer, Beuren Stuttgart, 2002.
[6] N. Re, A. Sgamellotti, C. Floriani, Organometallics 19 (2000) 1115.
[7] A. Marrone, N. Re, Organometallics 21 (2002) 3562.
[8] V. Cadierno, M.P. Gamasa, J. Gimeno, M. González-Cueva, E. Lastra, J. Borge, S. García-Granda, E. Pérez-Carreño, Organometallics 15 (1996) 2137.
[9] M.A. Esteruelas, A.V. Gómez, A.M. López, J. Modrego, E. Oñate, Organometallics 16 (1997) 5826.
[10] M. Baya, P. Crochet, M.A. Esteruelas, E. Gutiérrez-Puebla, A.M. López, J. Modrego, E. Oñate, N. Vela, Organometallics 19 (2000) 2585.
[11] R.F. Winter, K.-W. Klinkhammer, S. Záliš, Organometallics 20 (2001) 1317.
[12] D. Touchard, P. Haquette, A. Daridor, L. Toupet, P.H. Dixneuf, J. Am. Chem. Soc. 116 (1994) 11157.
[13] D. Péron, A. Romero, P.H. Dixneuf, Gazz. Chim. Ital. 124 (1994) 497.
[14] D. Péron, A. Romero, P.H. Dixneuf, Organometallics 14 (1995) 3319.
[15] D. Touchard, N. Pirio, L. Toupet, M. Fettouhi, L. Ouahab, P.H. Dixneuf, Organometallics 14 (1995) 5263.
[16] G. Roth, H. Fischer, Organometallics 15 (1996) 1139.
[17] G. Roth, H. Fischer, Organometallics 15 (1996) 5766.
[18] G. Roth, H. Fischer, T. Meyer-Friedrichsen, J. Heck, S. Houbrechts, A. Persoons, Organometallics 17 (1998) 1511.
[19] R.M. Bullock, J. Chem. Soc., Chem. Commun. (1989) 165.
[20] M.I. Bruce, Chem. Rev. 91 (1991) 107.
[21] I. de los Ríos, M.J. Tenorio, M.C. Puerta, P. Valerga, J. Am. Chem. Soc. 119 (1997) 6529.
[22] E. Peréz-Carreño, P. Paoli, A. Ienco, C. Mealli, Eur. J. Inorg. Chem. (1999) 1315.
[23] V. Cadierno, M.P. Gamasa, J. Gimeno, C. González-Bernardo, E. Pérez-Carreño, S. García-Granda, Organometallics 20 (2001) 5177.
[24] F. de Angelis, A. Sgamellotti, N. Re, Organometallics 21 (2002) 5944.
[25] J.R. Lomprey, J.P. Selegue, Organometallics 12 (1993) 616.
[26] M.I. Bruce, P. Hinterding, P.J. Low, B.W. Skelton, A.H. White, J. Chem. Soc., Chem. Commun. (1996) 1009.
[27] M.I. Bruce, P. Hinterding, P.J. Low, B.W. Skelton, A.H. White, J. Chem. Soc., Dalton Trans. (1998) 467.
[28] M.I. Bruce, P. Hinterding, M. Ke, P.J. Low, B.W. Skelton, A.H. White, Chem. Commun. (1997) 715.
[29] M.I. Bruce, M. Ke, B.D. Kelly, P.J. Low, M.E. Smith, B.W. Skelton, A.H. White, J. Organomet. Chem. 590 (1999) 184.
[30] R.F. Winter, Organometallics 16 (1997) 4248.
[31] R.F. Winter, Chem. Commun. (1998) 2209.
[32] R.F. Winter, Eur. J. Inorg. Chem. (1999) 2121.
[33] R.F. Winter, F.M. Hornung, Organometallics 18 (1999) 4005.
[34] R.F. Winter, S. Hartmann, S. Záliš, K.W. Klinkhammer, Dalton Trans. (2003) 2342.
[35] S. Hartmann, R.F. Winter, T. Scheiring, M. Wanner, J. Organomet. Chem. 637–639 (2001) 240.
[36] R.-C. Harbort, S. Hartmann, R.F. Winter, K.W. Klinkhammer, Organometallics 22 (2003) 3171.
[37] K. Venkatesan, F.J. Fernández, O. Blacque, T. Fox, M. Alfonso, H.W. Schmalle, H. Berke, Chem. Commun. (2003) 2006.
[38] K. Ilg, H. Werner, Angew. Chem. 112 (2000) 1691.
[39] F. Coat, M. Guillemot, F. Paul, C. Lapinte, J. Organomet. Chem. 578 (1999) 76.
[40] C.J. Adams, M.I. Bruce, B.W. Skelton, A.H. White, Chem. Commun. (1996) 2663.
[41] C.J. Adams, M.I. Bruce, B.W. Skelton, A.H. White, J. Organomet. Chem. 584 (1999) 254.
[42] V. Guillaume, P. Thominot, F. Coat, A. Mari, C. Lapinte, J. Organomet. Chem. 565 (1998) 75.
[43] P. Haquette, D. Touchard, L. Toupet, P. Dixneuf, J. Organomet. Chem. 565 (1998) 63.
[44] S. Hartmann, Synthese, Dissertation, Universität Stuttgart, 2003.
[45] E. Bustelo, M. Jimenez-Tenorio, K. Mereiter, M.C. Puerta, P. Valerga, Organometallics 21 (2002) 1903.
[46] A.G.M. Barrett, N. Carpenter, Organometallics 6 (1987) 2249.
[47] S. Jung, C.D. Brandt, H. Werner, New. J. Chem. 25 (2001) 1101.
[48] S. Rigaut, D. Touchard, P.H. Dixneuf, Organometallics 22 (2003) 3980.
[49] R. Castarlenas, P.H. Dixneuf, Angew. Chem. 115 (2003) 4662.
[50] H. Fischer, N. Szesni, G. Roth, N. Burzlaff, B. Weibert, J. Organomet. Chem. 683 (2003) 301.
[51] J.P. Selegue, Organometallics 1 (1982) 217.
[52] H. Le Bozec, K. Ouzzine, P.H. Dixneuf, J. Chem. Soc., Chem. Commun. (1989) 219.
[53] D. Pilette, K. Ouzzine, H. Le Bozec, P.H. Dixneuf, C.E.F. Rickard, W.R. Roper, Organometallics 11 (1992) 809.
[54] M.A. Esteruelas, A.V. Gómez, F.M. Lahoz, A.M. López, E. Oñate, L.A. Oro, Organometallics 15 (1996) 3423.
[55] M.A. Esteruelas, A.V. Gómez, A.M. López, J. Modrego, E. Oñate, Organometallics 17 (1998) 5434.
[56] J. Bernad, M.A. Esteruelas, A.M. López, J. Modrego, M.C. Puerta, P. Valerga, Organometallics 18 (1999) 4005.
[57] H. Fischer, D. Reindl, C. Troll, F. Leroux, J. Organomet. Chem. 490 (1995) 221.
[58] H. Werner, A. Stark, P. Steinert, C. Grünwald, J. Wolf, Chem. Ber. 128 (1995) 49.
[59] V. Cadierno, M.P. Gamasa, J. Gimeno, M.C. López-González, J. Borge, S. García-Granda, Organometallics 16 (1997) 4453.
[60] D. Touchard, P.H. Dixneuf, Coord. Chem. Rev. 178–180 (1998) 409.
[61] B. Buriez, D.J. Cook, K.J. Harlow, A.F. Hill, T. Welton, A.J.P. White, D.J. Williams, J.D.E.T. Wilton-Ely, J. Organomet. Chem. (1999) 264.
[62] C. Bianchini, N. Mantovani, L. Marvelli, M. Peruzzini, R. Rossi, A. Romerosa, J. Organomet. Chem. 617–618 (2001) 233.
[63] M.L. Buil, M.A. Esteruelas, A.M. López, E. Oñate, Organometallics 22 (2003) 162.
[64] N. Mantovani, L. Marvelli, R. Rossi, V. Bertolasi, C. Bianchini, I.D.L. Rios, M. Peruzzini, Organometallics 21 (2002) 2382.

[65] S. Rigaut, O. Maury, D. Touchard, P.H. Dixneuf, Chem. Commun. (2001) 373.
[66] W. Runge, in: S.R. Landor (Ed.), The Chemistry of Allenes: Stereochemical, Spectroscopic and Special Aspects, vol. 3, Academic Press, London, 1982.
[67] J.-L. Moreau, M. Gaudemar, J. Organomet. Chem. 108 (1976) 159.
[68] J.C. Craig, N.N. Ekwuribe, Tetrahedron Lett. 21 (1980) 2587.
[69] G. Maas, T. Mayer, Synthesis (1991) 1209.
[70] G. Pourcelot, P. Cadiot, Bull. Soc. Chim. Fr. (1966) 3024.
[71] M. Tamm, T. Jentzsch, W. Werncke, Organometallics 16 (1997) 1418.
[72] D. Touchard, N. Pirio, P.H. Dixneuf, Organometallics 14 (1995) 4920.
[73] H. Fischer, N. Szesni, Coord. Chem. Rev. 248 (2004) 1659.
[74] D. Lin-Vien, N.B. Colthup, W.G. Fateley, J.G. Grasselli, in: The Handbook of Infrared and Raman Characteristic Frequencies of Organic Molecules, Academic Press, San Diego, 1991.
[75] J. Manna, K.D. John, M.D. Hopkins, Adv. Organomet. Chem. 38 (1995) 79.
[76] I.-Y. Wu, J.T. Linn, J. Luo, C.-S. Li, C. Tsai, Y.S. Wen, C.-C. Hsu, F.-F. Yeh, S. Liou, Organometallics 17 (1998) 2188.
[77] R. Denis, L. Toupet, F. Paul, C. Lapinte, Organometallics 19 (2000) 4240.
[78] C. Bianchini, F. Laschi, D. Masi, F.M. Ottavani, A. Pastor, M. Peruzzini, F. Zanobini, J. Am. Chem. Soc. 115 (1993) 2723.
[79] C. Lin, T. Ren, E.J. Valente, J.D. Zubkowski, J. Organomet. Chem. 579 (1999) 114.
[80] A.J. Hodge, S.L. Ingham, A.K. Kakkar, M.S. Khan, J. Lewis, N.J. Long, D.G. Parker, P.R. Raithby, J. Organomet. Chem. 488 (1995) 205.
[81] I.R. Whittall, M.G. Humphrey, D.C.R. Hockless, B.W. Skelton, A.H. White, Organometallics 14 (1995) 3970.
[82] A.M. McDonagh, I.R. Whittall, M.G. Humphrey, B.W. Skelton, A.H. White, J. Organomet. Chem. 519 (1996) 229.
[83] M. Duetsch, F. Stein, R. Lackmann, E. Pohl, R. Herbst-Irmer, A.d. Meijere, Chem. Ber. 125 (1992) 2051.
[84] F. Stein, M. Duetsch, E. Pohl, R. Herbst-Irmer, A.D. Meijere, Organometallics 12 (1993) 2556.
[85] R. Aumann, K. Roths, R. Fröhlich, Organometallics 16 (1997) 5893.
[86] C. Rabiller, J.P. Renou, G.J. Martin, J. Chem. Soc., Perkin Trans. II (1977) 536.
[87] S. Conejero, J. Díez, M.P. Gamasa, J. Gimeno, S. García-Granda, Angew. Chem. 114 (2002) 3589.
[88] A. Wolinska, D. Touchard, P.H. Dixneuf, J. Organomet. Chem. 420 (1991) 217.
[89] E. Bustelo, M. Jiménez-Tenorio, M.C. Puerta, P. Valerga, Organometallics 18 (1999) 4563.
[90] M.P. Gamasa, J. Gimeno, C. González-Bernardo, J. Borge, S. García-Granda, Organometallics 16 (1997) 2483.
[91] K. Urtel, A. Frick, G. Huttner, L. Zsolnai, P. Kircher, P. Rutsch, E. Kaifer, A. Jacobi, Eur. J. Inorg. Chem. (2000) 33.
[92] A. Fürstner, M. Picquet, C. Bruneau, P.H. Dixneuf, Chem. Commun. (1998) 1315.
[93] B. Buriez, I.D. Burns, A.F. Hill, A.J.P. White, D.J. Williams, J.D.E.T. Wilton-Ely, Organometallics 18 (1999) 1504.
[94] M. Martín, O. Gevert, H. Werner, J, Chem. Soc., Dalton Trans. (1996) 2275.
[95] S. Jung, K. Ilg, C.D. Brandt, J. Wolf, H. Werner, Dalton Trans. (2002) 318.
[96] H. Werner, C. Grünwald, P. Steinert, O. Gevert, J. Wolf, J. Organomet. Chem. 565 (1998) 231.
[97] I. de los Ríos, M. Jiménez-Tenorio, M.C. Puerta, P. Valerga, J. Organomet. Chem. 549 (1997) 221.
[98] M.C. Colbert, J. Lewis, N.J. Long, P.R. Raithby, M. Younus, A.J.P. White, D.J. Williams, N.N. Payne, L. Yellowlees, D. Beljonne, N. Chawdhury, R.H. Friend, J. Chem. Soc., Dalton Trans. (1998) 3034.
[99] E. Bustelo, M. Jiménez-Tenorio, M.C. Puerta, P. Valerga, Eur. J. Inorg. Chem. (2001) 2391.
[100] V. Cadierno, M.P. Gamasa, J. Gimeno, E. Lastra, J. Borge, S. García-Granda, Organometallics 13 (1994) 745.
[101] H. Berke, G. Huttner, J.v. Seyerl, Z. Naturforsch. B 36B (1981) 1277.
[102] R.J.H. Clark, T.J. Dines, Angew. Chem. Int. Ed. Engl. 25 (1986) 131.
[103] J. van Slageren, R.F. Winter, A. Klein, S. Hartmann, J. Organomet. Chem. 670 (2003) 137.
[104] G.A. Olah, C.U. Pittman Jr., R. Waack, M. Doran, J. Am. Chem. Soc. 88 (1966) 1488.
[105] W. Runge, J. Firl, Ber. Bunsenges Phys. Chem. 79 (1975) 913.
[106] P.T. Czech, X.-Q. Ye, R.F. Fenske, Organometallics 9 (1990) 2016.
[107] G.A. Olah, R.J. Spear, P.W. Westerman, J.-M. Denis, J. Am. Chem. Soc. 98 (1974) 5855.
[108] G.A. Olah, A.L. Berrier, L.D. Field, G.K.S. Prakash, J. Am. Chem. Soc. 104 (1982) 1349.
[109] V.V. Krishnamurty, G.K.S. Prakash, P.D. Iyer, G.A. Olah, J. Am. Chem. Soc. 108 (1986) 1575.
[110] K. Komatsu, T. Takai, S. Aonuma, K.i. Takeuchi, Tetrahedron Lett. 29 (1988) 5157.
[111] R. Gleiter, I. Hyla-Kryspin, P. Binger, M. Regitz, Organometallics 11 (1992) 177.
[112] M.E. Stoll, S.R. Lovelace, W.E. Geiger, H. Schimanke, I. Hyla-Kryspin, R. Gleiter, J. Am. Chem. Soc. 121 (1999) 9343.
[113] L.F. Sczepura, J. Giambra, R.F. See, H. Lawson, T.S. Janik, A.J. Jircitano, M.R. Churchill, K.J. Takeuchi, Inorg. Chim. Acta 84 (1984) 91.
[114] M. Krejcik, M. Danek, F. Hartl, J. Electroanal. Chem. 317 (1991) 179.
[115] S. Hartmann, R.F. Winter, B.M. Brunner, B. Sarkar, A. Knödler, I. Hartenbach, Eur. J. Inorg. Chem. (2003) 876.
[116] B.E.R. Schilling, R. Hoffmann, D.L. Lichtenberger, J. Am. Chem. Soc. 101 (1979) 585.
[117] N.M. Kostic, R.F. Fenske, Organometallics 1 (1982) 974.
[118] C. Fonseca Guerra, J.G. Snijders, G. te Velde, E.J. Baerends, Theor. Chim. Acc. 99 (1998) 391.
[119] S.J.A. van Gisbergen, J.G. Snijders, E.J. Baerends, Comput. Phys. Commun. 118 (1999) 119.
[120] M.J. Frisch, G.W. Trucks, H.B. Schlegel, G.E. Scuseria, M.A. Robb, J.R. Cheeseman, V.G. Zakrzewski, J.A. Montgomery Jr., R.E. Stratmann, J.C. Burant, S. Dapprich, J.M. Millam, A.D. Daniels, K.N. Kudin, M.C. Strain, O. Farkas, J. Tomasi, V. Barone, M. Cossi, R. Cammi, B. Mennucci, C. Pomelli, C. Adamo, S. Clifford, J. Ochterski, G.A. Petersson, P.Y. Ayala, Q. Cui, K. Morokuma, D.K. Malick, A.D. Rabuck, K. Raghavachari, J.B. Foresman, J. Cioslowski, J.V. Ortiz, A.G. Baboul, B.B. Stefanov, G. Liu, A. Liashenko, P. Piskorz, I. Komaromi, R. Gomperts, R.L. Martin, D.J. Fox, T. Keith, M.A. Al-Laham, C.Y. Peng, A. Nanayakkara, C. Gonzalez, M. Challacombe, P.M.W. Gill, B. Johnson, W. Chen, M.W. Wong, J.L. Andres, C. Gonzalez, M. Head-Gordon, E.S. Replogle, J.A. Pople, Gaussian 98, Revision A.11, Gaussian. Inc., Pittsburgh, PA, 1998.
[121] D.E. Woon, T.H. Dunning Jr., J. Chem. Phys. 98 (1993) 1358.
[122] A. Bergner, M. Dolg, W. Kuechle, H. Stoll, H. Preuss, Mol. Phys. 80 (1993) 1431.
[123] D. Andrae, U. Häussermann, M. Dolg, H. Stoll, H. Preuss, Theor. Chim. Acta 77 (1990) 123.
[124] P.J. Stephens, F.J. Devlin, C.F. Cabalowski, M.J. Frisch, J. Phys. Chem. 98 (1994) 11623.
[125] A.D. Becke, Phys. Rev. A 38 (1988) 3098.
[126] J.P. Perdew, Phys. Rev. A 33 (1986) 8822.